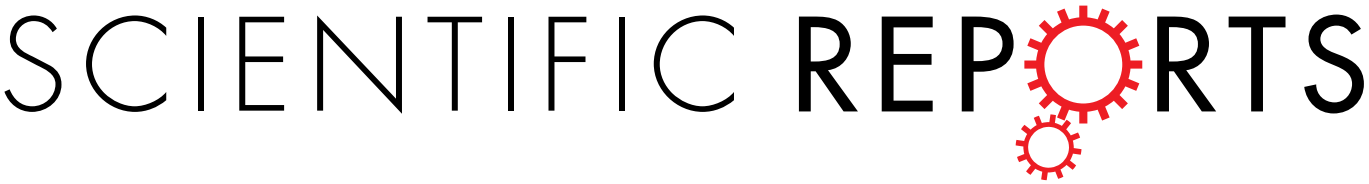

OPEN

Received: 30 August 2016
Accepted: 7 February 2017
Published online: 16 March 2017

Spatio-temporal dynamics of a planktonic system and chlorophyll distribution in a 2D spatial domain: matching model and data

Davide Valenti[1], Giovanni Denaro[2], Rosalia Ferreri[2], Simona Genovese[2], Salvatore Aronica[2], Salvatore Mazzola[2], Angelo Bonanno[2], Gualtiero Basilone[2] & Bernardo Spagnolo[1,3]

Field data on chlorophyll distribution are investigated in a two-dimensional spatial domain of the Mediterranean Sea by using for phytoplankton abundances an advection-diffusion-reaction model, which includes real values for physical and biological variables. The study exploits indeed hydrological and nutrients data acquired *in situ*, and includes intraspecific competition for limiting factors, i.e. light intensity and phosphate concentration. As a result, the model allows to analyze how both the velocity field of marine currents and the two components of turbulent diffusivity affect the spatial distributions of phytoplankton abundances in the Modified Atlantic Water, the upper layer of the water column of the Mediterranean Sea. Specifically, the spatio-temporal dynamics of four phytoplankton populations, responsible for about 80% of the total *chlorophyll a*, are reproduced. Results for phytoplankton abundances obtained by the model are converted in *chlorophyll a* concentrations and compared with field data collected in twelve marine sites along the Cape Passero (Sicily)- Misurata (Libya) transect. Statistical checks indicate a good agreement between theoretical and experimental distributions of chlorophyll concentration. The study can be extended to predict the spatio-temporal behaviour of the primary production, and to prevent the consequent decline of some fish species in the Mediterranean Sea.

During the last decades, the study of the spatio-temporal behaviour of phytoplankton abundance assumed a role of fundamental importance to predict the effects induced by physical and hydrological changes on the fish abundances in marine ecosystems[1–5]. In particular, field observations focused on the spatial distribution of chlorophyll concentration, which is the main marker of the phytoplankton populations[2,4–9]. These represent the base of the marine food web, and are used to estimate the biomass primary production in all aquatic ecosystems[4,10].

Theoretical models for population dynamics allowed to reproduce the spatio-temporal distributions of phytoplankton groups in a one-dimensional spatial domain by considering the effects of heterogeneity of the limiting factors along the water column[4,5,11–19]. On the other side, some authors introduced two- and three-dimensional models[20,21], in which the habitat of planktonic groups is considered homogenous for the nutrient and the environmental parameters are fixed constant in the whole ecosystem. In particular, these assumptions are connected with the lack of experimental data, whose availability is crucial for the estimation of some environmental variables[16,18], such as the light intensity, the velocity field of marine currents, the horizontal and vertical turbulent diffusivities. Moreover, unlike some one-dimensional models[4,5,15–18], the numerical results for phytoplankton abundances are not converted in chlorophyll concentration, and therefore the comparison between theoretical results and experimental data can not be performed. For these reasons, the theoretical chlorophyll concentration obtained by the phytoplankton abundances has been never reproduced in the vertical water plane of the marine ecosystems. In general, the analyses are usually carried out on the horizontal water plane by using the remote

[1]Dipartimento di Fisica e Chimica, Università di Palermo, Group of Interdisciplinary Theoretical Physics and CNISM, Unità di Palermo, Viale delle Scienze, Ed. 18, I-90128, Palermo, Italy. [2]Istituto per l'Ambiente Marino Costiero, CNR, U.O.S. di Capo Granitola, Via del Faro 3, I-91020, Campobello di Mazara, TP, Italy. [3]Istituto Nazionale di Fisica Nucleare, Sezione di Catania, Italy. Correspondence and requests for materials should be addressed to D.V. (email: davide.valenti@unipa.it)

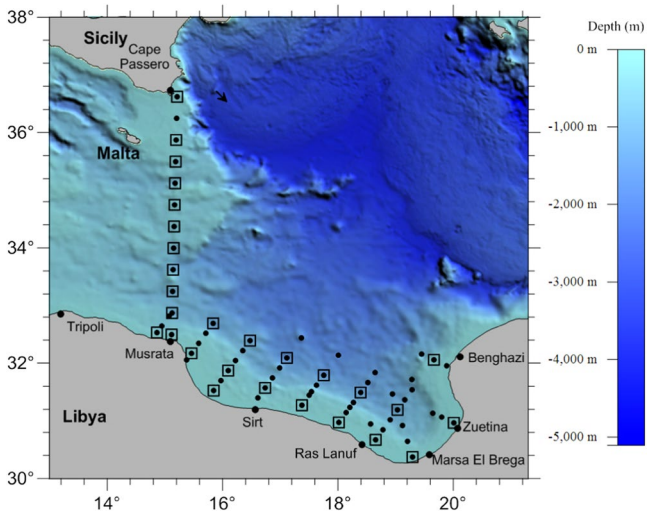

Figure 1. Location of the area investigated during the MedSudMed-08 cruise. The CTD stations are indicated by black circles and nutrient stations by empty squares. The bathymetry dataset was downloaded from the NOAA web portal (http://www.ngdc.noaa.gov/). Map was obtained by Surfer®[12] from Golden Software, LLC (www.goldensoftware.com).

sensing data[22,23], while it would be more useful to reproduce the field data collected in the vertical water plane, where the biodiversity of marine species can be investigated.

Here we introduce a more realistic two-dimensional model, which takes into account the physical and biochemical processes responsible for a strong spatial heterogeneity, typical of the Mediterranean Sea. This allows to reproduce the experimental spatial distributions of *chlorophyll a* (*chl a*) and *divinil chlorophyll a* (*Dvchl a*) concentration in the Strait of Sicily.

The sampling was carried out on a grid of 72 hydrographic profiles covering the Gulf of Syrte and the Strait of Sicily. In particular, our analysis focuses on the north-south transect (12 sites) crossing the eastern sill of the Strait of Sicily between Cape Passero and Misurata (see Fig. 1), characterized by the passage of superficial water masses in transit between the eastern and western basin of the Mediterranean Sea[24,25]. The bathymetry dataset used in Fig. 1 was downloaded from the NOAA web portal (http://www.ngdc.noaa.gov/)[26].

This area is interesting from a hydrological point of view since the surface marine currents of Atlantic origin, i.e. Atlantic Ionian Stream (AIS) and Atlantic Libyan Current (ALC), cause different environmental conditions for the phytoplankton growth between the Sicilian coast and Libyan coast. Moreover, the strong winds support the upwelling of nutrients close to the Sicilian coast. This favours the growth of phytoplankton populations also during the summer season when, on the contrary, it should be expected a decrease of the primary production of biomass due to the reduced water mixing. For these features, the whole area represents an important region for the spawning and growth of sardines and anchovies[7,27], and therefore for the fishery activities carried out in the Strait of Sicily[25].

In this work, a two-dimensional advection-reaction-diffusion model is used to reproduce, on a vertical "water plane", the spatio-temporal dynamics of four picophytoplankton populations. Specifically we consider the vertical "water plane" defined by the transect direction (x-axis) and the water surface-seabed direction (z-axis). The differential equations for the phytoplankton dynamics take into account the following contributions: (i) biomass production (birth and death); (ii) passive movement connected with turbulence and local transport; (iii) active movement of microorganisms along the water column.

The biomass primary production is described by a reaction term, which takes into account the nonlinear interactions between the growth of phytoplankton abundance and the two limiting factors[11,12,28,29], i.e. light intensity and nutrient concentration. Specifically, the decrease of the light intensity as a function of depth, associated with an opposite gradient for nutrients, allows each phytoplankton population to have a positive net growth rate within its production layer[4,5,18]. Accordingly, the magnitude and the position of the chlorophyll peaks within the two-dimensional spatial domain are strictly connected with the spatial distribution of the limiting factors[4,30], which however depend on the hydrological conditions of the transect investigated.

Regarding this point, it is worth to recall that the effects of mixing and local transport (passive movement) on the phytoplankton dynamics are taken into account by inserting in our equations diffusion and advection terms, respectively. Both terms are also included in the differential equation for the nutrient dynamics in order to well reproduce the two-dimensional distribution of phosphate concentration along the transect. By this way, in our analysis we consider both the direct effects of the hydrological and physical variables on the spatio-temporal behaviour of all phytoplankton groups, and those indirectly induced by the non-linear interactions between phytoplankton and the nutrient dynamics. These effects on the phytoplankton dynamics have been investigated previously in horizontal water planes[22]. However, the role of hydrological and physical variables has never been studied in a vertical water plane, where vertical chlorophyll profiles, and eventual deep chlorophyll maxima (DCMs), can be observed and analyzed. Moreover, our study presents three further novelties compared

to previous investigations based on advection-diffusion-reaction models: (i) the two horizontal components of the velocity field are those measured in the transect during the oceanographic survey (15–30 July 2008); (ii) the vertical turbulent diffusivity is estimated on the basis of the Pacanowski and Philander model[31,32], by using the experimental data collected *in situ*; (iii) the horizontal turbulent diffusivity is fixed according to the theoretical results presented in previous works[31,33].

Finally, the active movement of each planktonic group is considered by using a taxis term, which depends on the behaviour of the net growth rate along the water column in accordance with previous studies[4,5,11].

On this theoretical basis, we devise an advection-diffusion-reaction model which allows to reproduce the map of *chlorophyll a* concentration in the two-dimensional spatial domain of the Cape Passero-Misurata transect. Here, the hydrological parameters guarantee oligotrophic conditions during the summer season, with phosphates being the nutrient component which plays the role of limiting factor for the phytoplankton growth[4,5,16–18,24,34].

In the following, first we consider four picophytoplankton populations[35–39], i.e. Synechococcus, Prochlorococcus (HL-ecotype), Prochlorococcus (LL-ecotype) and the whole picoeukaryotes domain, which are the main groups in the Strait of Sicily (see Supplementary Information). Then we present a two-dimensional advection-reaction-diffusion model, obtaining the spatio-temporal dynamics for the phytoplankton abundances of these populations.

As a second step, we convert the phytoplankton abundances, expressed in $cells/m^3$, into *chl a* and *Dvchl a* concentrations, expressed in $\mu g/dm^3$, by using the experimental cellular content measured by Vaulet and Courties, and the conversion curves obtained by Brunet *et al.*[36,40].

As a third step, the vertical chlorophyll distributions extracted from the theoretical map are compared with the corresponding experimental profiles collected during MedSudMed-08 oceanographic survey (15–30 July 2008), by performing statistical checks based on the χ^2 test. Then, the results of these statistical tests are compared with those obtained by the "full" version of the model, in which all biological parameters are fixed (see Supplementary Information). Finally, a qualitative comparison between numerical results and experimental data is also performed for the average phosphate concentration and the average chlorophyll concentration in the Modified Atlantic Water (MAW).

Results

The theoretical distributions of phytoplankton abundance for the four populations were obtained by solving numerically Eqs (1–7). In our analysis we considered half-saturation constants varying as a function of the position, x, along the transect, so that Eqs (1–7) form a "reduced" model[41], i.e. a model with some free parameters respect to the full version, where all parameters are fixed.

In this work, the numerical method used, whose computer implementation consists in a C++ program, exploits an explicit finite difference scheme. More specifically, we used a technique based on the Method of Lines (MOL) approach, where space and time discretizations are considered separately. This method was useful to combine various discretizations for the diffusion, advection and taxis terms together with the non-linear reaction term. Indeed, we solved the differential equations of the model by performing a centered-in-space differencing for the diffusion terms, and a third-order upwind-biased differencing for the advection and taxis terms. The increment of the spatial variables is set at 5.0 km for the x-direction and 2.0 m for the z-direction, while the time step is fixed at 0.05 h. In particular, these values are chosen such as to get stability conditions for the numerical method used. On the other side, the stability analysis, performed according to previous works[20,42–44], indicates that the convergence of our algorithm is guaranteed[20,42,44].

As initial conditions, we assumed for each picophytoplankton group a low cell concentration uniformly distributed within the domain studied in agreement with Ryabov *et al.*[45], while the phosphate concentrations are fixed equal to those measured along the water column in the sampling sites.

In order to obtain the steady spatial distributions, we solved numerically our equations over a time interval ($t_{max} = 2 \cdot 10^4 h$) long enough to reach the stationary solution[4,18,46].

In Fig. 2 we show the four picophytoplankton abundance distributions obtained by the reduced model within the two-dimensional domain. Here, it is possible to observe the presence of the abundance peak for Synechococcus and Prochlorococcus HL in shallower and intermediate layers of MAW, in correspondence of the Sicilian–Maltese shelf and the Libyan coast. Conversely, the Prochlorococcus LL abundance is very low in both the coastal zones, while an abundance peak of picoeukaryotes is mainly observed in intermediate layers of the MAW between Cape Passero and Malta. Moreover, the theoretical results indicate that the Prochlorococcus LL dominate the marine ecosystem between the Medina Sill and the Libyan coast, showing their abundance peak in deeper layers of the MAW, where the other groups are absent.

In general, from a quantitative point of view, these findings are in agreement with experimental data collected in the Strait of Sicily during the last years[24,35,36]. Specifically, the analysis of the numerical results shows that the average concentrations and the abundance peaks of all phytoplankton groups studied are in very good agreement with the experimental findings obtained in the Sicilian - Maltese shelf by Brunet *et al.*[35,36] during a previous oceanographic survey.

According to previous studies[4,16,18], to compare the theoretical results with the experimental findings, the phytoplankton abundances obtained by the model are converted into *chl a* and *Dvchl a* concentrations, setting the cellular content of Synechococcus equal to 1.18 fg *chl a* $cell^{-1}$[40], and using the curves of mean vertical profile for the other groups[35,36]. Furthermore, we add these converted theoretical results with the contribute of chlorophyll concentration, $\Delta b_{(Dv)chla}$, due to the presence of nano- and micro-phytoplankton ($>3\,\mu m$), which accounts for 20% of the total quantity of *chl a* and *Dvchl a*. This contribution is uniformly distributed along the MAW (z-axis), but changes along the Cape Passero–Misurata transect (x-axis) (see Fig. 1), taking on different values in the 12 different marine sites analyzed. We reproduce therefore the horizontal distribution of the chlorophyll contribute $\Delta b_{(Dv)chla}(x)$ by calculating the 20% of fluorescence data acquired in each hydrological station, and interpolating

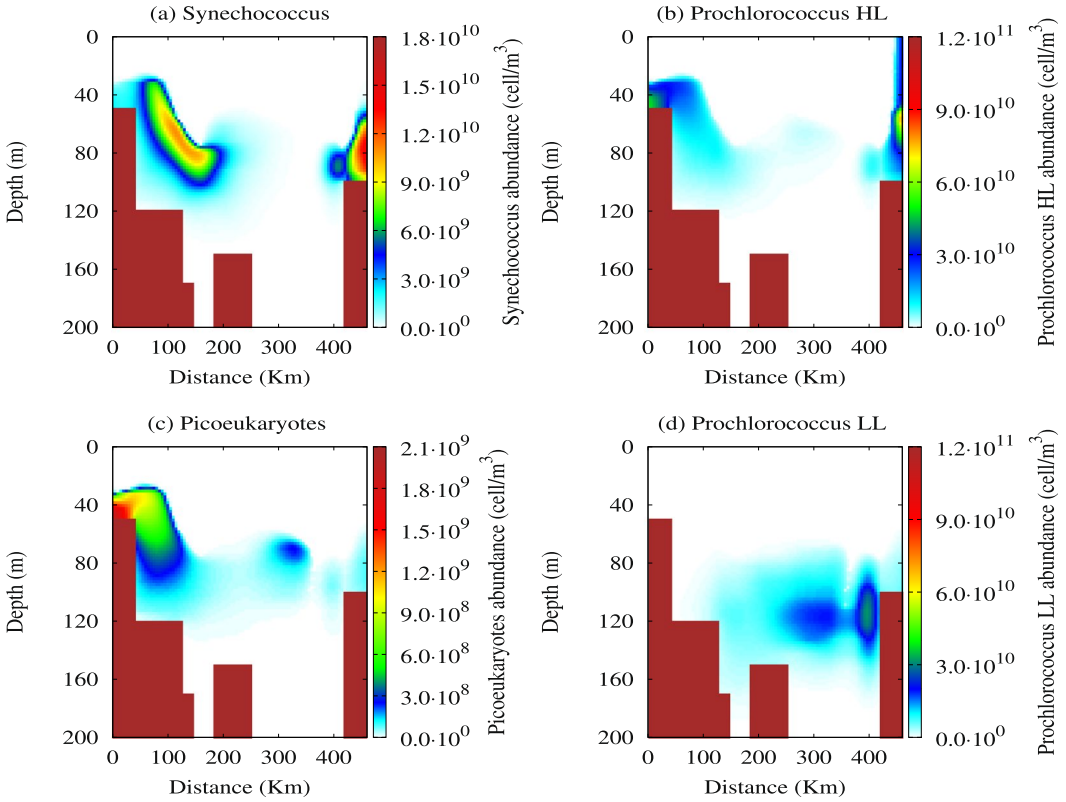

Figure 2. Two-dimensional distribution of the four picophytoplankton populations obtained by the reduced model. The contour maps show the cell concentrations of (**a**) Synechococcus, (**b**) Prochlorococcus HL concentrations, (**c**) picoeukaryotes and (**d**) Prochlorococcus LL at the steady state. The values of the parameters used in the reduced model are those shown in Table 1 of Supplementary Information.

the results obtained for all sampling sites of the transect. On the basis of these assumptions, we obtain the spatio-temporal behaviour of the total *chl a* and *Dvchl a* concentration for the whole domain investigated.

The theoretical results of the *(Dv)chl a* concentrations of the four picophytoplankton groups, the total *chl a* and *Dvchl a* concentration and the phosphate concentration in stationary conditions are shown in Fig. 3. Here, we observe that the presence of high chlorophyll concentration in both the coastal zones is mainly due to Synechococcus and Prochlorococcus HL, in accordance with the theoretical results obtained for the picophytoplankton abundances (see Fig. 2). Although Synechococcus and Prochlorococcus HL prevail in the coastal zones, these two groups do not contribute significantly to the total *chl a* and *Dvchl a* concentration in the remaining part of the Cape Passero–Misurata transect. Indeed, the theoretical results indicate that the most part of chlorophyll concentration is due to the presence of picoeukaryotes and Prochlorococcus LL, which prevail in the Strait of Sicily during the summer season, when the oligotrophic conditions guarantee higher light intensity in deeper layers of the water column. In particular, these two groups dominate the marine ecosystem between the Sicilian coast and the Libyan coast in correspondence of the deep chlorophyll maximum (DCM). More specifically, the chlorophyll peak for picoeukaryotes is localized along the whole transect in the intermediate layers of the MAW, while that for Prochlorococcus LL is only obtained between the Medina Sill and the Libyan coast in deeper layers of the water column. These results are in a good agreement with the experimental findings obtained for each phytoplankton group by other authors[35–38].

We also compare the steady spatial distribution for the total *chl a* and *Dvchl a* concentration and the phosphate concentration obtained by the model with the experimental data collected during the MedSudMed-08 oceanographic survey (see Fig. 4). From a qualitative point of view, the theoretical results for the total *chl a* and *Dvchl a* concentration are in a good agreement with experimental data in the whole transect except in a restricted area localized off the Libyan coast, and a sampling site (M2) located close to Cape Passero (see Fig. 5). These discrepancies are due to the high values taken on by the zonal component (horizontal and perpendicular to the transect) of the geostrophic currents. Our analysis, based on a two-dimensional model, does not allow indeed to include effects due to current component along the third spatial direction (y-axis). Finally, the comparison between the theoretical distributions and the experimental data shows a good agreement for the nutrient concentration in the whole domain, except in the hydrological stations localized close to Medina Sill. Here, in the intermediate layers of the MAW, the phosphate concentration obtained by the reduced model is overestimated respect to the values detected by the field observations. However, this behaviour can be explained by an approximative estimation of the horizontal turbulent diffusivity used within the area confined between the Sicilian coast and the Medina Sill (see the Supplementary Information).

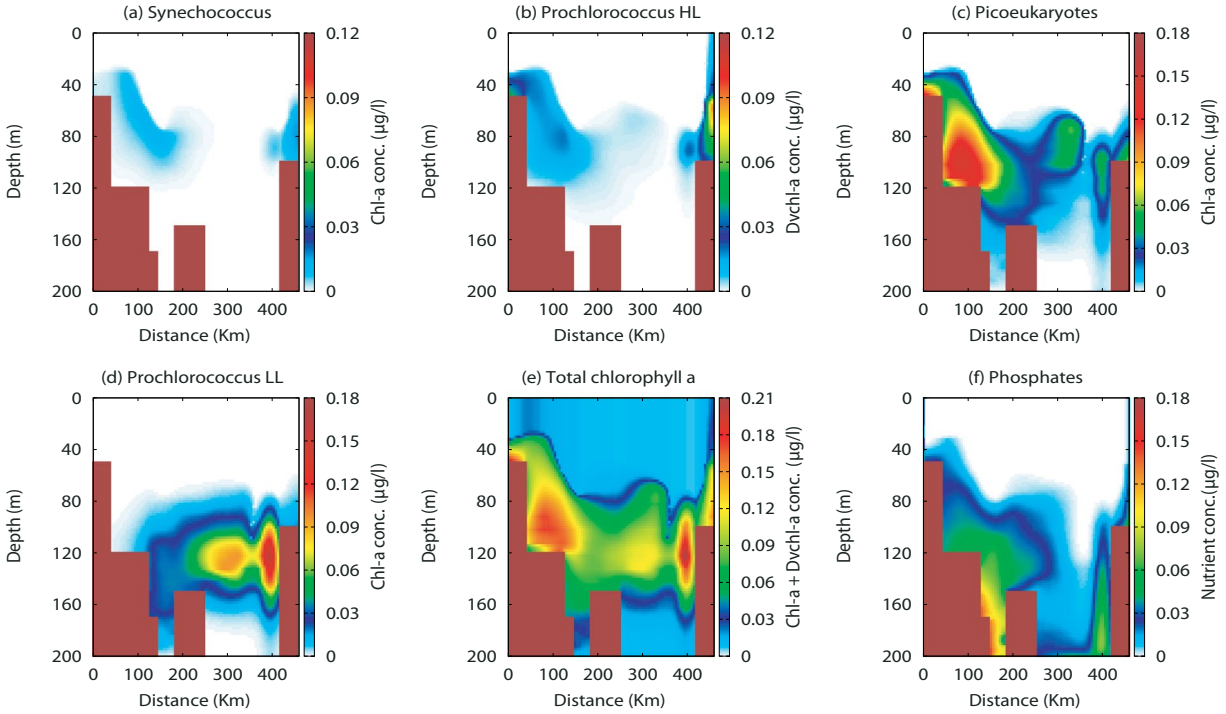

Figure 3. Theoretical spatial distribution of *chl a* and *Dvchl a* concentrations and phosphate concentration. The contour maps show the content of chlorophyll for (**a**) Synechococcus, (**b**) Prochlorococcus HL, (**c**) picoeukaryotes, (**d**) Prochlorococcus LL, (**e**) all phytoplankton groups, and (**f**) the phosphate concentration in the marine ecosystem investigated (Cape Passero–Misurata transect). The values of the parameters used in the reduced model are those shown in Table 1 of Supplementary Information.

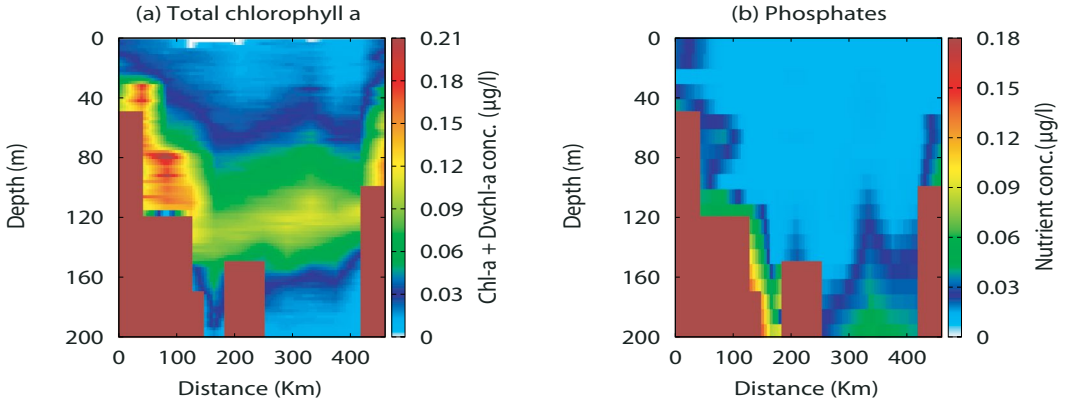

Figure 4. Spatial distribution of the *chlorophyll a* and phosphate concentrations obtained by the field observations. The contour maps for (**a**) the total *chl a* and *Dvchl a* concentration and (**b**) the phosphate concentration were obtained by interpolating the experimental data acquired in the twelve hydrological stations of the Cape Passero (Sicily)- Misurata (Libya) transect, during the MedSudMed-08 oceanographic survey.

In Fig. 5 we compare the experimental profiles of *chlorophyll a* concentration with the corresponding theoretical vertical distributions extracted from the contour maps obtained by the reduced model at the steady state. Here we observe a good qualitative agreement between experimental data (green line) and numerical results (red points) in all hydrological stations investigated. We also perform a quantitative analysis, based on the goodness-of-fit test χ^2, for the 12 stations of the transect. The results of the χ^2 test, shown in Table 2 of Supplementary Information, indicate a very good agreement between theoretical and experimental chlorophyll profiles in the hydrological stations (*M6*-*M9*) localized in the central part of the Strait of Sicily, where the geostrophic currents take on the same direction of the transect. The best reduced chi-square ($\tilde{\chi}^2_{red} = 0.0021$) is observed in the station *M12*, close to the Libyan coast, where the magnitude of the geostrophic current components is very low. In other sampling sites, the results of χ^2 test indicate a worse agreement between theoretical and experimental profiles, even if the reduced chi-square $\tilde{\chi}^2$ takes on values comparable with those obtained in previous works, where one-dimensional models were used to study the phytoplankton dynamics in summer season[4,

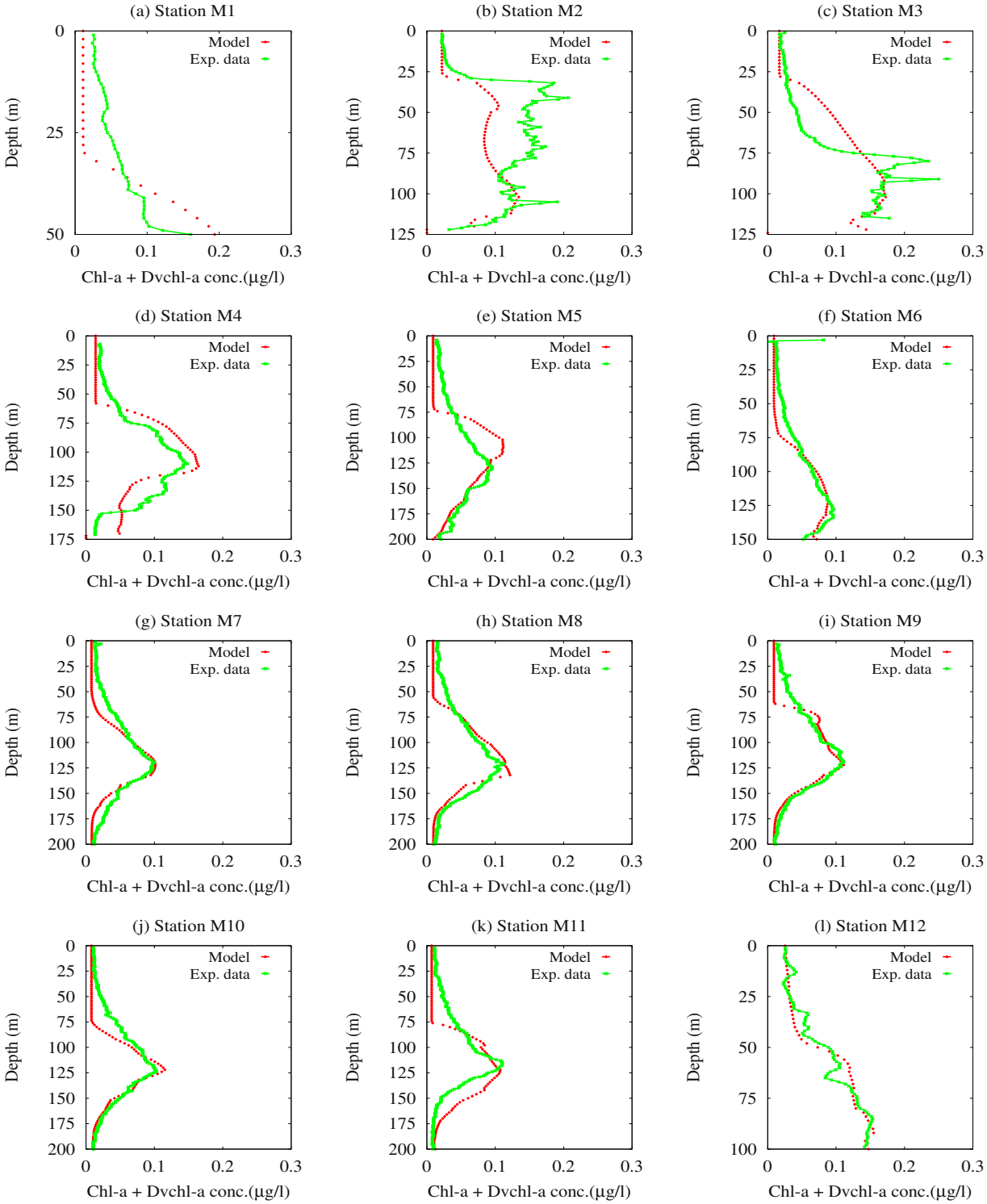

Figure 5. Theoretical distributions (red points) and experimental profiles (green line) of the total *chl a* and *Dvchl a* concentration. The numerical results, obtained by the reduced advection-diffusion-reaction model, are compared with the experimental data collected in the twelve hydrological stations of the Cape Passero (Sicily)-Misurata (Libya) transect, during the MedSudMed-08 oceanographic survey.

[16]. On the whole, the two-dimensional model represents therefore an improvement compared to the corresponding one-dimensional model, because it provides a high-resolution map of the *chlorophyll a* distribution in a good agreement with the experimental findings collected in the 12 marine stations analyzed.

To better investigate and understand the effects of the environmental parameters on the chlorophyll distributions in the marine ecosystem studied, we analyze for the reduced model the theoretical values of the magnitude, depth and width of the DCM in all hydrological stations placed along the Cape Passero -Misurata transect. The

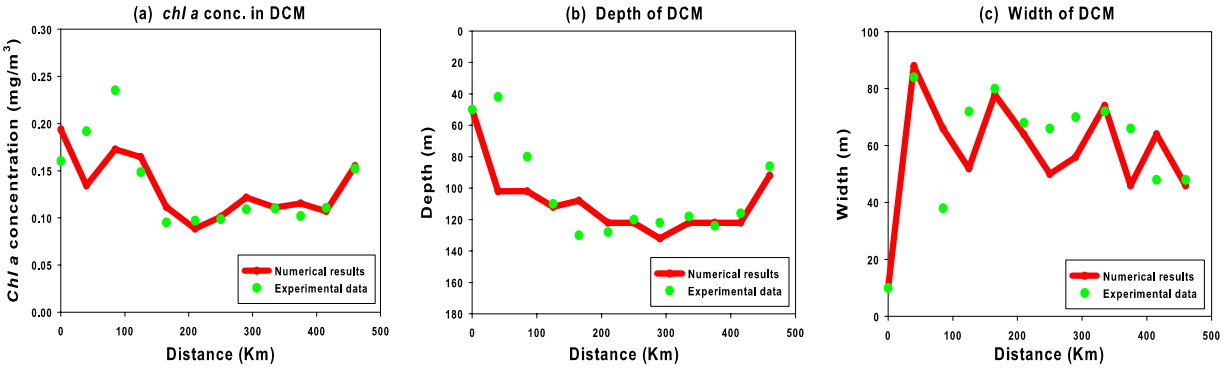

Figure 6. Magnitude (panel a), depth (panel b), and width (panel c) of the DCM as a function of the distance from the Cape Passero. The red lines, with a spatial resolution of 5 Km, reproduce the behaviour of the DCM obtained by the reduced model along the Cape Passero–Misurata transect. The green points describe the behaviour of the DCM obtained by the experimental data collected in the twelve hydrological stations of the transect during the sampling period (15^{th}–30^{th} July 2008).

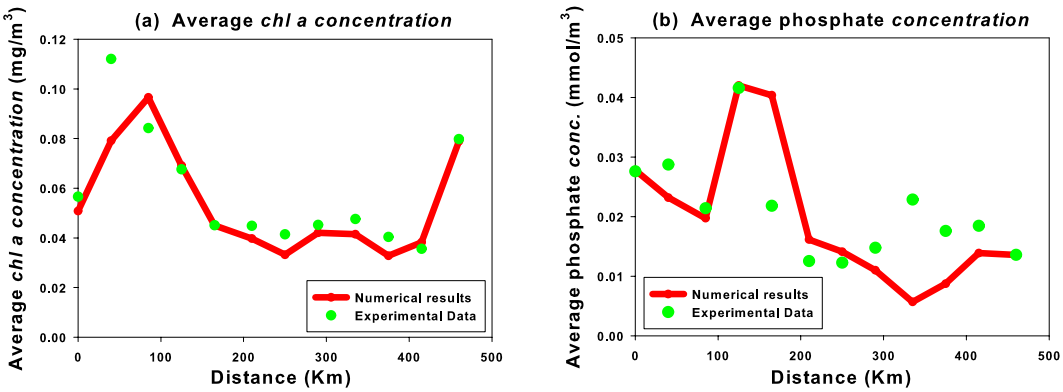

Figure 7. Average total *chl a* concentration and phosphate concentration as a function of the distance from the Cape Passero. Red lines show, with a spatial resolution of 5 Km, the average concentrations in the MAW obtained by the reduced model along the Cape Passero–Misurata transect. The green points are the average concentrations in the MAW obtained by the experimental data collected in correspondence of the twelve hydrological stations of the transect during the sampling period (15^{th}–30^{th} July 2008).

results, shown in Fig. 6, indicate that the magnitude and depth of the DCM take on a nonmonotonic behaviour along the transect, while showing, for the most part of the stations, a clear correlation with the nutrient concentration obtained by the reduced model. In particular, we observe that the *chl a* concentration in the DCM takes on higher values in marine sites located close to the Sicilian and Lybian coasts, where larger values of the horizontal and the vertical turbulent diffusivities generate an increase of the phosphate concentration. Conversely, after a rapid decrease between Malta and the Medina Sill, the magnitude of the DCM takes on lower values in the middle of the Strait of Sicily, in accordance with the behaviour of the phosphate concentration observed in this area, characterized by lower values of the turbulent diffusivities.

Moreover, the numerical results show that, close to the coastal zones, the DCM is quite shallow because of a high phosphate concentration, while it is quite deep between the stations *M*5 and *M*11, where the oligotrophic conditions are guaranteed by lower turbulent diffusivities. On the whole, the theoretical results for the magnitude and depth of DCM are in a good agreement with the experimental ones, except in two stations (*M*2 and *M*3) located close to the Sicilian coast.

The analysis performed for the width of the DCM indicates that the experimental findings are well reproduced by the reduced model only in hydrological stations close to the coastal zones. Conversely, the width of DCM is mostly underestimated respect to the field observations in the hydrological stations localized in the middle of the Strait of Sicily. This result is connected with the difficulty to determine the correct values for the horizontal and vertical turbulent diffusivities. Finally, unlike other analysis performed on advection-diffusion-reaction models[15–18], in this study we do not observe a connection between the magnitude and width of the DCM.

In Fig. 7, we analyze the effects of the mixing and the local transport on the average concentration of *chlorophyll a* and phosphate within the Cape Passero -Misurata transect. Here, the theoretical results indicate that the hydrological conditions in the coastal zones generate the rising of the nutrients in the shallower layers of the MAW, causing an enhancement of the average chlorophyll concentration. In particular, an average chlorophyll peak is observed between the Sicilian coast and the Medina Sill (station *M*3), while another peak is present close

to the Libyan coast (station *M*12). In the first case, the upwelling of the nutrients and the consequent growth of the phytoplankton biomass are due to the combined effect of the Atlantic Ionian Stream (AIS) and a higher water mixing. In the second case, the increase of average chlorophyll concentration is mainly due to the presence of the Atlantic Libyan Current (ALC), which carries nutrients from the Gulf of Syrte. Conversely, the reduced mixing between the Medina Sill and the Libyan coast causes in the MAW very low values of average phosphate concentration and, as a consequence, of chlorophyll concentration. In general, we observe for the average chlorophyll concentration a good agreement between the numerical results and experimental findings along the whole transect, except in the station *M*2. On the other hand, the average phosphate concentration is well reproduced close to the coastal zones, while some differences are observed in the hydrological stations localized in the middle of the transect.

In conclusion, the analysis performed in this section shows that the discrepancies between theoretical and experimental *chlorophyll a* distributions can be ascribed to: (i) the lack of experimental data on the horizontal turbulent diffusivity, necessary to better estimate the effects of high turbulence close to the coastal zones; (ii) the difficulty to determine the correct value for the vertical turbulent diffusivity in the upwelling regions; (iii) the necessity to neglect the zonal component (perpendicular to the transect) of the geostrophic velocity, because of the two-dimensional structure of the model; (iv) the lack of experimental data for the half-saturation coefficients of all picophytoplankton groups involved in our study. Moreover, the contribution of the nano- and micro-phytoplankton fraction to the total chlorophyll concentration could be underestimated close to the Sicilian coast, where the high nutrient concentration could be responsible for the growth of diatoms and Dinophytes.

Anyway, the results presented in this section indicate that the two-dimensional model provides, in wide areas of the marine ecosystem, spatial distributions of *chlorophyll a* concentration which fit quite well the field observations.

Discussion

In this work we presented an innovative study on the spatio-temporal dynamics of phytoplankton in a marine ecosystem located in the Strait of Sicily. Initially, we performed an analysis on the two-dimensional distributions of chlorophyll and phosphate concentration obtained from data sampled, during the summer season, in twelve hydrological stations, located along the Cape Passero–Misurata transect. Here, field observations indicate the presence of a strong spatial heterogeneity in physical and chemical variables such as velocity field, water density, and nutrient concentration. Moreover, we observed that the characteristics of the vertical chlorophyll profile in each sampling site are strictly connected with the horizontal velocities of marine currents, turbulent diffusivities (vertical and horizontal), and nutrient concentration at the boundaries of the ecosystem.

In this work we used a two-dimensional advection-reaction-diffusion model, while neglecting the terms of the local transport in the direction perpendicular to the transect, since in the most hydrological stations investigated during the summer period the velocity field is parallel to the transect, and the contribution of the zonal geostrophic velocity on the local transport can be therefore neglected (see Supplementary Information and, in particular, Fig. 1).

The equations of the reduced model were solved by numerical methods, simulating the spatio-temporal dynamics of four phytoplankton populations, responsible for about 80% of the total *chlorophyll a* inside the Modified Atlantic Water, that is the upper layer of the water column of the Mediterranean Sea. Then, by using the conversion rates obtained in previous works[36,40] we obtained the *chl a* and *Dvchl a* theoretical concentrations, and compared them with the corresponding field data.

The spatio-temporal dynamics of the four planktonic populations was obtained by the model equations, taking into account explicitly the effects of environmental variables. More in detail, we considered the different hydrological features of the 12 stations along the transect investigated. In particular, we found that the strong stratification of the Mediterranean Sea in the summer season[2,47,48] causes a reduced nutrient concentration in the shallower layers of the MAW, and therefore a low chlorophyll concentration in the most part of the Strait of Sicily (except in the coastal zones). Conversely, the strong wind at the marine surface induces the upwelling of nutrients close to the Sicilian coast, while favouring the growth of phytoplankton populations also during the summer season. Moreover, an increase of the chlorophyll concentration is also observed close to Libyan coast due to the presence of the Atlantic Libyan Current (ALC), which carries nutrients from the Gulf of Syrte.

We note also that in our equations the effects of the mixing, local transport (passive movement), and non-linear interactions between phytoplankton and nutrient dynamics are modeled by the diffusion and advection terms. Moreover, our model exploits values of hydrological and physical variables experimentally measured, including horizontal components of the velocity field and vertical turbulent diffusivity obtained from field observations.

These aspects represent a novelty within the landscape of the modeling of phytoplankton dynamics in a vertical water plane. Moreover, the model provides a tool for a better and deeper understanding of the role played by hydrological conditions on the spatial distribution of phytoplankton abundances, which represent the base of the food web for marine ecosystems. Our theoretical findings indeed could be used to analyze the role of environmental variables, through the modifications induced in the phytoplankton distributions, in the dynamics of zooplankton populations and fish species in the Strait of Sicily[7,25,27,49]. Indeed previous investigations showed that the anchovy population prevails in the upwelling region[3,49,50], where the high nutrient concentrations favour the growth of larger size phytoplankton groups, which are at the basis of the food chain of this fish species. On the other hand, sardines, which are able to capture smaller size phytoplankton and zooplankton, dominate geographical areas with reduced water mixing during the most part of the year[50].

In our analysis, we considered the presence of two limiting factors responsible for the competition among the four picophytoplankton populations modeled. The biological parameters were set to values typical of these planktonic groups, according to previous field observations carried out in the Strait of Sicily[10,29,35,36,51–58]. Specifically,

environmental conditions were fixed according to field observations, and biological parameters were set in such a way to guarantee, along the water column, the coexistence of all four populations[4,5,12,16–18,45].

Moreover, the heterogeneous composition of each picophytoplankton population showed a spatial variability, modeled by varying the values of half-saturation constants along the transect analyzed. About this, our modeling actually pays the lack of an adequate knowledge of the mechanism used by phytoplankton cells to absorb nutrient molecules and energy from the marine waters under the different environmental conditions[9]. Indeed, a correct modeling of phytoplankton dynamics should also take into account that the half-saturation constants depend on the nutrient concentration and the light intensity, which change as a function of the position (x, z) within the two-dimensional domain. However, a preliminary analysis (results here not reported) based on the full model has been performed, obtaining spatial distributions of phytoplankton abundances in a quite good agreement (except in stations M1, M2, M3) with the field data acquired along the Cape Passero - Misurata transect.

Anyway, due to the characteristics of the marine ecosystem analyzed (see Supplementary Information), in view of better reproducing the experimental data, we assumed half-saturation constants as space dependent parameters. So we used a reduced model in which the values of half-saturation constants depend on the position x along the transect, instead of the full model where all biological parameters are fixed. In particular, the values of half-saturation constants for each station were initially fixed in such a way that the boundaries of the production layer of each population are localized at depths determined according to the theoretical expression by Ryabov *et al.*[14,45]. The final values of half-saturation constants were obtained by using an iterative procedure, based on χ^2 test, which optimizes the theoretical profiles of chlorophyll distributions compared with those obtained by field data (see Supplementary Information). Moreover, in our analysis we imposed an additional constraint: in all hydrological stations the theoretical abundances (cell concentrations) for each phytoplankton population have to be in a good agreement with those experimentally observed by Brunet *et al.*[35,36]. Our theoretical results satisfy also this condition.

In our analysis the theoretical 2D distribution of chlorophyll concentration was obtained by exploiting the conversion curves[36]. Then we extracted from the chlorophyll map the theoretical chlorophyll profiles, comparing them with the experimental profiles collected in the 12 stations during the MedSudMed-08 oceanographic survey (15–30 July 2008). At this stage we applied the above cited optimization procedure, obtaining theoretical profiles in a good agreement with those obtained from field observations, and strongly dependent on the hydrological variables (horizontal velocities and turbulent diffusivities), characterized by different values in the various stations analyzed. Moreover, from a qualitative point of view, we observed that the magnitude, depth and width of the DCMs predicted by the reduced model match quite well those obtained by field observations. We also calculated, in each station, the average chlorophyll concentration along the water column, finding a good agreement between theoretical results and experimental data in the whole transect, except in station $M2$. Finally, the good agreement between predicted results and experimental data for the average phosphate concentration represented a further validation of the reduced model proposed.

We also compared quantitatively theoretical and experimental chlorophyll profiles, performing the χ^2 goodness-of-fit test. The results showed that the best reduced chi-square is obtained for the hydrological stations localized between the Medina Sill and the Libyan coast, where the turbulent diffusivities take on low values and the geostrophic currents are parallel to the direction of the transect. Conversely, the worst values of χ^2 are obtained between the Sicilian coast and the Medina Sill, where the high vertical turbulent diffusivity triggers the upwelling of nutrient from deeper layers, and the direction of the marine currents is not parallel to the transect.

Afterwards, we also compared the results of the χ^2 test for the reduced and full models, by using the Akaike Information Criterion and the Cohen's effect size measure[41,59]. In particular, both statistical checks show that also the full model is able to well reproduce the experimental chlorophyll profiles in the most part of the transect, even if the best χ^2 values are obtained by the reduced model. As a final remark we note that, from a conceptual point of view it appears more correct to use the reduced model, which takes into account the spatial variability of the half-saturation constants. These parameters indeed depend strongly on the environmental conditions, such as water turbidity which influences the light intensity along the water column, and nutrient concentration. The reduced model allows to take into account this dependence by including site specific values for half-saturation constants. Finally, the small values of the Cohen's effect size measure allows to extend to the full model the good agreement between experimental and theoretical distributions of chlorophyll, obtained when the reduced model is used.

In general, this study indicates that the advection-diffusion-reaction model proposed is able to reproduce correctly the spatial distributions of the chlorophyll concentration, when biological and environmental parameters are set to values typical (experimentally measured) of the ecosystem considered (Strait of Sicily). Anyway, it is expected that the theoretical distributions for chlorophyll concentration could be improved by using a 3D model, which should allow to take into account the effects of diffusion and advection along the third dimension (perpendicularly to the transect), here not considered because of the 2D structure of the experimental dataset. In particular, the implementation of the 3D model would allow to obtain a better agreement between the theoretical results and the experimental data in the hydrological stations where the velocity field is not parallel to the transect. Moreover, a better modeling needs a deeper knowledge of biological and environmental parameters such as: (i) horizontal and vertical turbulent diffusivities close to coastal zones; (ii) dependence of the half-saturation constants on the spatial distributions of nutrient concentration and light intensity; (iii) real contribution of the nano- and micro-phytoplankton fraction to the chlorophyll concentration in the coastal zones; (iv) the inflow and outflow of nutrients and chlorophyll coming from the boundaries of the marine ecosystem.

In conclusion, the model proposed in this work appears as a valid candidate to predict the chlorophyll spatial distribution in marine ecosystems characterized by heterogeneous environmental conditions. Specifically, our findings indicate that the model is able to reproduce phytoplankton dynamics in aquatic ecosystems with different levels of eutrophication. We note that this model can be extended, including higher trophic levels such

as zooplankton populations, in view of reproducing and predicting the spatio-temporal behaviour of fish populations[5,21]. Finally, we wish to notice how the model and, more in general, the whole approach proposed represent a powerful tool to analyze and predict the effects of global warming on phytoplankton dynamics, in view of preventing the decline of the primary production in marine ecosystems[9,18].

Materials and Methods

Environmental data. The experimental data were collected in the period 15^{th}–30^{th} July 2008 during the MedSudMed-08 Oceanographic Survey carried out in the Central Mediterranean Sea (CMED) on board the CNR R/V Urania. This area was investigated by using a grid of 72 hydrographic profiles, which covered the Gulf of Syrte and a north-south transect crossing the eastern sill of the Strait of Sicily between Cape Passero and Misurata[24](see Fig. 1). Specifically, the sampling sites were located on a grid of 12×12 nautical miles in the Gulf of Syrte. The distance between two consecutive sites was about 22.5 nautical miles along the Cape Passero-Misurata transect. Hydrological conditions remained constant for the entire sampling period and were representative of the oligotrophic Mediterranean Sea in summer.

For each sampling site, continuous vertical profiles of conductivity, temperature, density and pressure were collected from the surface to the bottom of the water column by means of a CTD-rosette system, consisting of a CTD SBE 911 plus probe (Sea-Bird Inc.), and a General Oceanics rosette with 24 Niskin Bottles[24,60]. Simultaneously, the *chlorophyll a* fluorescence data (*chl a* concentration in μg/l) were acquired by using the Chelsea Aqua 3 sensor mounted on the probe. All parameters were processed, generating for each site a text file, in which the experimental values are given with a 1 m step[16–18].

The vertical profiles of the two horizontal components of the current velocity have been acquired by using a Lowered Acoustic Doppler Current Profiler system (LADCP) and computed by applying the Lamont-Doherty Earth Observatory (LDEO) processing software[61]. At the same time, the main surface circulation patterns were evaluated by the Absolute Dynamic Topography during the investigated period.

The horizontal velocities were collected in all sampling sites of the transect except in the station *M*12. Here, we assumed that the velocities were the same as in the nearest station *L*2718. Indeed, we recall that the vertical profiles of horizontal marine currents and water density were necessary to estimate the spatial distribution of the vertical turbulent diffusivity[31,32] along the whole Cape Passero-Misurata transect (see Supplementary Information).

The seawater samples to perform the dissolved inorganic nutrients measurements were collected during the oceanographic survey at standard depths in all hydrological stations of the transect investigated except in the M2 site. The nutrient samples were stored at $-20\,°C$ without carrying out any preliminary filtration. Nitrite, nitrate, silicate and phosphate concentrations were measured successively in laboratory by using a Brän-Luebbe AutoAnalyzer, and following classical methods with slight modifications[24,62].

The model. The dynamics of the primary production of biomass is studied by using an advection-diffusion-reaction model[4,11,12,45]. In particular, we investigate the spatio-temporal behaviour of four picophytoplankton populations, which interact with each other indirectly through the competition for light intensity and nutrient concentration. By solving the equations of the model, we obtain the steady spatial distribution of cell concentration for the populations analyzed in the Strait of Sicily, i.e. Synechococcus, Prochlorococcus HL, picoeukaryotes, and Prochlorococcus LL, indicated by $b_1(x, z, t)$, $b_2(x, z, t)$, $b_3(x, z, t)$, and $b_4(x, z, t)$, respectively. Here, $b_i(x, z, t)$ denotes the phytoplankton abundance (cells per unit volume) of *i-th* population in the position (x, z) within the two-dimensional domain at time t. Moreover, the spatial distributions of the phosphate concentration $R(x, z, t)$ and light intensity $I(x, z, t)$ are obtained. In our study, the domain is composed by the sum of seven rectangular subdomains, which reproduce the bathymetric profile of the transect together with the vertical boundaries localized in the two hydrological stations close to the two coasts. Specifically, z represents the depth of the water column from the surface ($z=0$) to the bottom ($z=z_b$) of each subdomain, while x indicates the distance from the Sicilian coast, measured from Cape Passero ($x=0$) to Misurata ($x_i=0$) along the transect.

The dynamics of the picophytoplankton abundance is modeled by including three processes[11,12,20]: (i) net growth (reaction term); (ii) active/passive movement (taxis/advection term); (iii) movement due to turbulence (diffusion term).

The reaction term describes how the limiting resources affect the net phytoplankton growth rate ($G_i(x, z, t)$)[11,14,28,45,63,64], which depends on the balance between the gross production rate per capita and the mortality. In particular, the gross production rates are given by $\min\left\{f_{I_i}(I), f_{R_i}(R)\right\}$, where $f_{I_i}(I)$ and $f_{R_i}(R)$ are obtained by the Michaelis-Menten formulas for light intensity and phosphate concentration[4,16,18,19], while the mortality due to respiration, death, and grazing is described by the specific loss rates (m_i).

The taxis term provides a realistic description of motility skills of the planktonic groups, and depends on the swimming velocity v_i of each population, which is a function of the gradient of the net growth rate ($\partial G_i(x, z, t)/\partial z$)[11]. In particular, this function is defined as $v_i = + v_i^s$(sinking phytoplankton) if $\partial G_i(x, z, t)/\partial z > 0$, $v_i = -v_i^s$ (buoyant phytoplankton) if $\partial G_i(x, z, t)/\partial z < 0$, and $v_i = 0$ (motionless phytoplankton) if $\partial G_i(x, z, t)/\partial z = 0$, where v_i^s is a constant parameter, whose value (positive) is calculated for each population according to Raven[51].

The non-active movement of all phytoplankton groups depends on the turbulence (diffusion term) and the local transport (advection term) of biomass[4,20,45]. In particular, the diffusion term reproduces the effects of the turbulence on the two-dimensional distribution of phytoplankton groups through the horizontal ($D_h(x)$) and the vertical ($D_v(x, z)$) turbulent diffusivities, which change as a function of the depth (z) and the length (x), while remaining constant with the time. Hence, as a preliminary step, we obtain the values of vertical turbulent diffusivity from field observations by exploiting the model devised by Pacanowski and Philander[31]. The horizontal turbulent diffusivity is fixed in accordance with values estimated by other authors[31,33,65] (see Supplementary Information).

The advection term allows to describe the effects on the picophytoplankton distributions induced by the horizontal velocity component ($v_h(x, z)$) of the marine currents along the x-direction. Since in the most part of the transect the velocity field is parallel to the x-direction (see Supplementary Information and, in particular, Fig 1), we do not parameterize the local transport of nutrients and chlorophyll along the y-direction due to the zonal geostrophic velocity. The horizontal velocities (constant in time) are calculated by using the experimental data collected during the oceanographic MedSudMed-08 survey (see Supplementary Information).

The phosphate concentration $R(x, z, t)$ is further increased by the recycling process of the dead phytoplankton. Moreover, the effects of the local transport and turbulence, responsible for the mixing of nutrients in the 2D domain, are taken into account by inserting in the differential equation for the phosphate concentration an advection term and two diffusion terms, respectively.

Finally, the light intensity $I(x, z, t)$ is assumed to depend on the site considered along the transect, and to decrease exponentially with the depth z, according to the Lambert-Beer's law[4,29,66,67].

Thus, the four-population model is defined by the following equations:

$$\begin{aligned}\frac{\partial b_i(x,\,z,\,t)}{\partial t} &= b_i\left(min\left(f_{I_i}(I), f_{R_i}(R)\right) - m_i\right) + \frac{\partial}{\partial z}\left[D_v(x,\,z)\frac{\partial b_i(x,\,z,\,t)}{\partial z}\right] \\ &+ \frac{\partial}{\partial x}\left[D_h(x)\frac{\partial b_i(x,\,z,\,t)}{\partial x}\right] - \frac{\partial}{\partial x}[v_h(x,\,z)b_i(x,\,z,\,t)] \\ &- \frac{\partial}{\partial z}[v_i(x,\,z,\,t)b_i(x,\,z,\,t)]\end{aligned} \tag{1}$$

$$\begin{aligned}\frac{\partial R(x,\,z,\,t)}{\partial t} &= -\sum\frac{b_i(x,\,z,\,t)}{Y_i}\cdot min\left(f_{I_i}(I), f_{R_i}(R)\right) + \frac{\partial}{\partial z}\left[D_v(x,\,z)\frac{\partial R(x,\,z,\,t)}{\partial z}\right] \\ &+ \frac{\partial}{\partial x}\left[D_h(x)\frac{\partial R(x,\,z,\,t)}{\partial x}\right] - \frac{\partial}{\partial x}[v_h(x,\,z)R(x,\,z,\,t)] \\ &+ \sum\varepsilon_i m_i\frac{b_i(x,\,z,\,t)}{Y_i}\end{aligned} \tag{2}$$

$$I(x,\,z,\,t) = I_{in}(x)\exp\left\{-\int_0^z\left[\sum a_i\cdot chl\ a_i(x,\,Z,\,t) + a_{bg}\right]dZ\right\}, \tag{3}$$

with i = 1, ..., 4. Here, ε_i, m_i, $1/Y_i$, and a_i are the nutrient recycling coefficient, the specific loss rate, the nutrient content, and the *chl a*-normalized average absorption coefficient of the *i-th* picophytoplankton population, respectively; a_{bg} is the background turbidity; $I_{in}(x)$ is the incident light intensity at the water surface, taking on different values along the transect (x-direction).

Respect to the phytoplankton populations the marine ecosystem is closed[20], that is we assume that no biomass can enter or leave the area investigated. Therefore, we fix the biomass fluxes to vanish at the boundaries of the domain:

$$[D_v(x,\,0)\frac{\partial b_i}{\partial z} - v_i b_i]|_{z=0} = 0, \qquad [D_v(x,\,z_b)\frac{\partial b_i}{\partial z} - v_i b_i]|_{z=z_b} = 0, \tag{4}$$

$$[D_h(0)\frac{\partial b_i}{\partial x} - v_h b_i]|_{x=0} = 0, \qquad [D_h(x_l)\frac{\partial b_i}{\partial x} - v_h b_i]|_{x=x_l} = 0. \tag{5}$$

For the nutrient (phospates) we assume: (i) no nutrient flux through the water surface; (ii) nutrient concentration at the other three boundaries fixed equal to the values measured during the oceanographic survey. Therefore, we set the phosphate fluxes at the boundaries of the domain as follows:

$$\frac{\partial R}{\partial z}|_{z=0} = 0, \qquad R(x,\,z_b) = R_{in}(x,\,z_b). \tag{6}$$

$$R(0,\,z) = R_{in}(0,\,z), \qquad R(x_l,\,z) = R_{in}(x_l,\,z). \tag{7}$$

Equations (1–7) represent the two-dimensional advection-diffusion-reaction model used to describe and reproduce the spatio-temporal dynamics of phytoplankton abundance.

References

1. Bopp, L. *et al.* Potential impact of climate change on marine export production. *Global. Biogeochem. Cy* **15**, 81–99 (2001).
2. Patti, B. *et al.* Role of physical forcings and nutrient availability on the control of satellite-based chlorophyll *a* concentration in the coastal upwelling area of the Sicilian Channel. *Sci. Mar.* **74(3)**, 577–588 (2010).
3. Bonanno, A. *et al.* Influence of environmental variability on anchovy early life stages (*Engraulis encrasicolus*) in two different areas of the Central Mediterranean Sea. *Hydrobiologia* **701**, 273–287 (2013).
4. Valenti, D., Denaro, G., Spagnolo, B., Conversano, F. & Brunet, C. How diffusivity, thermocline and incident light intensity modulate the dynamics of deep chlorphyll maximum in Tyrrhenian Sea. *PLoS ONE* **10(1)**, e0115468 (2015).
5. Valenti, D. *et al.* The role of noise on the steady state distributions of phytoplankton populations. *J. Stat. Mech* **2016**, 054044 (2016).
6. Jennings, S., Kaiser, M. J. & Reynolds, J. D. *Marine Fisheries Ecology*. (Blackwell Science: Oxford, 2001).

7. Cuttitta, A. *et al.* Anchovy egg and larval distribution in relation to biological and physical oceanography in the Strait of Sicily. *Hydrobiologia* **503**, 117–120 (2003).
8. Weston, K., Fernand, L., Mills, D. K., Delahunty, R. & Brown, J. Primary production in the deep chlorophyll maximum of the central North Sea. *J. Plankton Res.* **27**, 909–922 (2005).
9. Kiørboe, T. *A mechanistic approach to plankton ecology* (Princeton University Press, 2008).
10. Veldhuis, M. J. W., Timmermans, K. R., Croot, P. & Van Der Wagt, B. Picophytoplankton; a comparative study of their biochemical composition and photosynthetic properties. *J. Sea Res.* **53**, 7–24 (2005).
11. Klausmeier, C. A. & Litchman, E. Algal games: the vertical distribution of phytoplankton in poorly mixed water columns. *Limnol. Oceanogr.* **46**, 1998–2007 (2001).
12. Huisman, J., Thi, N. N. P., Karl, D. M. & Sommeijer, B. Reduced mixing generates oscillations and chaos in the oceanic deep chlorophyll maximum. *Nature* **439**, 322–325 (2006).
13. Ryabov, A. B. & Blausius, B. Population growth and persistence in a heterogeneous environment: the role of diffusion and advection. *Math. Model. Nat. Phenom* **3**, 42–86 (2008).
14. Ryabov, A. Phytoplankton competition in deep biomass maximum. *Theor. Ecol* **5**, 373–385 (2012).
15. Valenti, D. *et al.* Picophytoplankton dynamics in noisy marine environment. *Acta Phys. Pol. B* **43**, 1227–1240 (2012).
16. Denaro, G. *et al.* Spatio-temporal behaviour of the deep chlorophyll maximum in Mediterranean Sea: Development of a stochastic model for picophytoplankton dynamics. *Ecol. Complex.* **13**, 21–34 (2013).
17. Denaro, G. *et al.* Stochastic dynamics of two picophytoplankton populations in a real marine ecosystem. *Acta Phys. Pol. B* **44**, 977–990 (2013).
18. Denaro, G. *et al.* Dynamics of two picophytoplankton groups in Mediterranean Sea: Analysis of the deep chlorophyll maximum by a stochastic advection-reaction-diffusion model. *PLoS ONE* **8(6)**, e66765 (2013).
19. Valenti, D. *et al.* Stochastic models for phytoplankton dynamics in Mediterranean Sea. *Ecol. Complex.* **27**, 84–103 (2016).
20. Thi, N. N. P., Huisman, J. & Sommeijer, B. P. Simulation of three-dimensional phytoplankton dynamics: competition in light-limited environments. *J. Comput. Appl. Math.* **174**, 57–77 (2005).
21. Liu, Q. X., Jin, Z. & Li, B. L. Resonance and frequency-locking phenomena in spatially extended phytoplankton-zooplankton system with additive noise and periodic forces. *J. Stat. Mech.-Theory Exp* **5**, P05011 (2008).
22. Hernández-Carrasco, I., Rossi, V., Hernández-Garca, E., Garçon, V. & López, C. The reduction of plankton biomass induced by mesoscale stirring: A modelling study in the Benguela upwelling. *Deep-Sea Res. I* **83**, 65–80 (2014).
23. Falcini, F. *et al.* The Role of Hydrodynamics Processes on Anchovy Eggs and Larvae Distribution in the Sicily Channel (Mediterranean Sea): A Case Study for the 2004 Data Set. *PLoS ONE* **10(4)**, e0123213 (2015).
24. Placenti, F. *et al.* Water masses and nutrient distribution in the Gulf of Syrte and between Sicily and Libya. *J. Marine Syst.* **121–122**, 36–46 (2013).
25. Rinaldi, E., Buongiorno Nardelli, B., Volpe, G. & Santoleri, R. Chlorophyll distribution and variability in the Sicily Channel (Mediterranean Sea)as seen by remote sensing data. *Cont. Shelf Res.* **77**, 61–68 (2014).
26. Amante, C., Eakins, B. W. ETOPO1 1 Arc-Minute Global Relief Model: Procedures, Data Sources and Analysis. NOAA Technical Memorandum NESDIS NGDC-24 (National Geophysical Data Center NOAA, USA, 2009).
27. Agostini, V. N. & Bakun, A. 'Ocean triads' in the Mediterranean Sea: physical mechanisms potentially structuring reproductive habitat suitability (with example application to European anchovy, *Engraulis encrasicolus*). *Fish. Oceanogr.* **11**, 129–142 (2002).
28. Klausmeier, C. A., Litchman, E. & Levin, S. A. A model of flexible uptake of two essential resources. *J. Theor. Biol.* **246**, 278–289 (2007).
29. Hickman, A., Dutkiewicz, S., Williams, R. & Follows, M. Modelling the effects of chromatic adaptation on phytoplankton community structure in the oligotrophic ocean. *Mar. Ecol. Prog. Ser.* **406**, 1–17 (2010).
30. Norberg, J. Biodiversity and ecosystem functioning: a complex adaptive systems approach. *Limnol. Oceanogr.* **49**, 1269–1277 (2004).
31. Pacanowski, R. C. & Philander, S. G. H. Parameterization of Vertical Mixing in Numerical Models of Tropical Oceans. *J. Phys. Oceanogr.* **11**, 1443–1451 (1981).
32. Peters, H., Gregg, M. C. & Toole, J. M. On the parameterization of Equatorial Turbulence. *J. Geophys. Res.* **93**, 1199–1218 (1988).
33. Massel, S. R. *Fluid Mechanics for Marine Ecologists* (Springer-Verlag, Berlin Heidelberg, 1999).
34. Ribera d'Alcalà, M., Civitarese, G., Conversano, F. & Lavezza, R. Nutrient ratios and fluxes hint at overlooked processes in the Mediterranean Sea. *J. Geophys. Res.* **108(C9)**, 8106 (2003).
35. Brunet, C., Casotti, R., Vantrepotte, V., Corato, F. & Conversano, F. Picophytoplankton diversity and photoacclimation in the Strait of Sicily (Mediterranean Sea) in summer. I. Mesoscale variations. *Aquat. Microb. Ecol.* **44**, 127–141 (2006).
36. Brunet, C., Casotti, R., Vantrepotte, V. & Conversano, F. Vertical variability and diel dynamics of picophytoplankton in the Strait of Sicily, Mediterranean Sea, in summer. *Mar. Ecol. Prog. Ser.* **346**, 15–26 (2007).
37. Garczarek, L. *et al.* High vertical and low horizontal diversity of *Prochlorococcus* ecotypes in the Mediterranean Sea in summer. *FEMS Microbiol Ecol* **60**, 189–206 (2007).
38. Mella-Flores, D. *et al.* Is the distribution of Prochlorococcus and Synechococcus ecotypes in the Mediterranean Sea affected by global warming? *Biogeosciences* **8(9)**, 2785–2804 (2011).
39. La Ferla, R. *et al.* Vertical distribution of the prokaryotic cell size in the Mediterranean Sea. *Helgol. Mar. Res.* **66(4)**, 635–650 (2012).
40. Morel, A., Ahn, Y. H., Partensky, F., Vaulot, D. & Claustre, H. *Prochlorococcus* and *Synechococcus*: A comparative study of their optical properties in relation to their size and pigmentation. *J. Mar. Res.* **51**, 617–649 (1993).
41. Newsom, J. T. *Longitudinal Structural Equation Modeling: A Comprehensive Introduction*. (Routledge: New York, NY, 2015).
42. Roache, P. J. *Fundamentals of Computational Fluid Dynamics*. (Hermosa Publishers: Albuquerque, New Mexico, 1998).
43. Tveito, A. & Winther, R. *Introduction to Partial Differential Equations: A Computational Approach*. (Springer-Verlag: New York, 1998).
44. Hundsdorfer, W. & Verwer, J. G. *Numerical solution of time-dependent advection-diffusion-reaction equations publisher*. (Springer-Verlag: Berlin, 2003).
45. Ryabov, A. B., Rudolf, L. & Blasius, B. Vertical distribution and composition of phytoplankton under the influence of an upper mixed layer. *J. Theor. Biol.* **263**, 120–133 (2010).
46. Fennel, K. & Boss, E. Subsurface maxima of phytoplankton and chlorophyll: Steady-state solutions from a simple model. *Limnol. Oceanogr.* **48**, 1521–1534 (2003).
47. Behrenfeld, M. J. *et al.* Climate-driven trends in contemporary ocean productivity. *Nature* **444**, 752–755 (2006).
48. Barale, V., Jaquet, J. M. & Ndiaye, M. Algal blooming patterns and anomalies in the Mediterranean Sea as derived from the SeaWiFS data set (1998–2003). *Remote Sens. Environ.* **112**, 3300–3313 (2008).
49. Basilone, G. *et al.* Effect of habitat conditions on reproduction of the European anchovy (*Engraulis encrasicolus*) in the Strait of Sicily. *Fish. Oceanogr* **15**, 271–280 (2006).
50. D'Alelio, D., Libralato, S., Wyatt, T. & Ribera d'Alcalá, S. Ecological-network models link diversity, structure and function in the plankton food-web. *Sci. Rep* **6**, 21806 (2016).
51. Raven, J. A. The twelfth tansley lecture. Small is beautiful: the picophytoplankton. *Funct. Ecol* **12**, 503–513 (1998).
52. Raven, J. A., Finkel, Z. V. & Irwin, A. J. Picophytoplankton: bottom-up an top-down controls on ecology and evolution. *J. Geophys. Res.* **55**, 209–215 (2005).

53. Dimier, C., Brunet, C., Geider, R. & Raven, J. Growth and photoregulation dynamics of the picoeukaryote *Pelagomonas calceolata* in fluctuating light. *Limnol. Oceanogr.* **54**, 823–836 (2009).
54. Thingstad, T. F. & Sakshaugh, E. Control of phytoplankton growth in nutrient recycling ecosystems. Theory and terminology. *Mar. Ecol. Prog. Ser.* **63**, 261–272 (1990).
55. Quevedo, M. & Anadón, R. Protist control of phytoplankton growth in the subtropical north-east Atlantic. *Mar. Ecol. Prog. Ser.* **221**, 20–38 (2001).
56. Moore, L. R., Goericke, R. & Chisholm, S. W. Comparative physiology of synechococcus and prochlorococcus: influence of light and temperature on growth, pigments, fluorescence and absorptive properties. *Mar. Ecol. Prog. Ser.* **116**, 259–275 (1995).
57. Bertilsson, S., Berglund, O., Karl, D. M. & Chisholm, S. W. Elemental composition of marine *Prochlorococcus* and *Synechococcus*: implications for the ecological stoichiometry of the sea. *Limnol. Oceanogr.* **48**, 1721–1731 (2003).
58. Timmermans, K. R., van der Wagt, B., Veldhuis, M. J. W., Maatman, A. & de Baar, H. J. W. Physiological responses of three species of marine pico-phytoplankton to ammonium, phospahte, iron and light limitation. *J. Sea Res.* **53**, 109–120 (2005).
59. Akaike, H. Factor analysis and AIC. *Psychometrika* **52**, 317–332 (1987).
60. Bonanno, A. *et al.* Variability of water mass properties in the Strait of Sicily in summer period of 1998–2013. *Ocean Sci.* **10**, 759–770 (2014).
61. Visbeck, M. Deep velocity profiling using lowered acoustic Doppler current profilers: bottom track and inverse solutions. *J. Atmos. Ocean. Technol.* **19(5)**, 794–807 (2002).
62. Grasshoff, K., Kremling, K., Ehrhardt, M. *Methods of Seawater Analysis* (Wiley-Vch Verlag, Weinheim, Germany, 1999).
63. Mei, Z. P., Finkel, Z. V. & Irwin, A. J. Light and nutrient availability affect the size-scaling of growth in phytoplankton. *J. Theor. Bio* **259**, 582–588 (2009).
64. Bougaran, G., Bernard, O. & Sciandra, A. Modeling continuous cultures of microalgae colimited by nitrogen and phosphorus. *J. Theor. Biol.* **265**, 443–454 (2010).
65. Katz, E. J., Bruce, J. G. & Petrie, B. D. Salt and mass flux in the Atlantic Equatorial Undercurrent. *Deep-Sea Res* **26**, 139–160 (1979).
66. Shigesada, N. & Okubo, A. Effects of competition and shading in planktonic communities. *J. Math. Biol.* **12**, 311–326 (1981).
67. Kirk, J. T. O. *Light and Photosynthesis in Aquatic Ecosystems* (2nd edition) (Cambridge University Press, 1994).

Acknowledgements

Authors acknowledge the financial support by Ministry of University, Research and Education of Italian Government, Project "RITMARE SP2_WP1_AZ3_UO04– Potenziamento delle campagne scientifiche di acquisizione di informazioni indipendenti dalla pesca sulle risorse", the FAO Project MedSudMed "Assessment and Monitoring of the Fishery Resources and the Ecosystems in the Straits of Sicily", funded by the Italian Ministry MIPAAF, and PON02_00451_3362121 "PESCATEC–Sviluppo di una Pesca Siciliana Sostenibile e Competitiva attraverso l'Innovazione Tecnologica".

Author Contributions

R.F., S.G., S.A., S.M., A.B. and G.B. conceived and designed the experiments; R.F., S.G., S.A., S.M., A.B. and G.B. performed the experiments; D.V. G.D. B.S. analyzed the data; R.F., S.G., S.A., S.M., A.B. and G.B. contributed reagents/materials/analysis tools; D.V., G.D. and B.S. wrote the paper; D.V., G.D. and B.S. designed the software used to solve numerically the equations of the system. All authors contributed to review the manuscript.

Additional Information

Supplementary information accompanies this paper at doi:10.1038/s41598-017-00112-z

Competing Interests: The authors declare no competing financial interests.

Publisher's note: Springer Nature remains neutral with regard to jurisdictional claims in published maps and institutional affiliations.

SUPPLEMENTARY INFORMATION

Spatio-temporal dynamics of a planktonic system and chlorophyll distribution in a 2D spatial domain: matching model and data

Davide Valenti[a], Giovanni Denaro, Rosalia Ferreri, Simona Genovese, Salvatore Aronica, Salvatore Mazzola, Angelo Bonanno, Gualtiero Basilone, Bernardo Spagnolo

Correspondence should be addressed to D.V. (email: davide.valenti@unipa.it)

SUPPLEMENTARY METHODS

Analysis of environmental data

The vertical distributions of hydrological parameters, i.e. temperature and salinity, were used to identify the different water masses present in the studied area [1, 2]. Here, the field observations indicate the presence of the Modified Atlantic Water (MAW), i.e. the upper layer of the water column of Atlantic origin localized from the surface down to 200 m. In particular, the MAW is placed above the Levantine Intermediate Water (LIW), i.e. the intermediate layer of the Mediterranean basin, and includes the euphotic zone of the water column populated by picophytoplankton groups. Moreover, the surface circulation pattern allowed to single out the presence of two main branches of the MAW which cross the Cape Passero-Misurata transect at the water surface: (i) Atlantic Ionian Stream (AIS) localized between the Sicilian coast and Malta; (ii) Atlantic Libyan Current placed close to the Libyan coast. As a consequence, the horizontal velocities take on the same direction of the transect between the Medina Sill and the Libyan coast, while assume a direction non-parallel to the transect close to Cape Passero and Misurata (see Fig. 1 in Supplementary Figures).

The vertical profiles of fluorescence along the whole transect, between the surface and 200 m of depth, indicate that the total *chlorophyll a* concentration takes on the highest values close to the Sicilian coast, due to the strong influence of the thermohaline front present over the Sicilian - Maltese shelf [1, 2]. In the rest of the section, the deep chlorophyll maximum (DCM) is less pronounced and is located between 100 and 150 m of depth. Specifically, the total *chl a* concentration ranges between 0.095 and 0.235 μg *chl a* l^{-1} along the whole transect. Moreover, differences among the twelve hydrological stations are observed in the

shape and width of the DCM.

The chemical analysis performed on the bottle samples confirms that the Mediterranean Sea is a phosphorus limited basin due to the high N:P ratio measured along the water column in all sites investigated [1, 3]. Specifically, the phosphate concentration takes on very low values due to the absorption of Saharan dust, while the higher concentration of nitrate, nitrite and ammonium are strictly connected to: (i) the excess of nitrogen fixation in the Mediterranean basin, (ii) the nutrient flow coming from the coasts.

Phytoplankton properties

In this work, the contribution of each picophytoplankton group to the total amount of chlorophyll is based on the experimental estimation of cellular *chlorophyll a* content obtained by performing the high-performance liquid chromatography (HPLC) analysis on the seawater samples collected between Cape Passero and Malta during a previous oceanographic survey [4, 5].

According to the study carried out in the Mediterranean Sea by other authors [4–7], the phytoplankton community can be divided into three main size fractions: pico- ($< 3\mu m$), nano- ($3-20\mu m$) and micro-phytoplankton ($> 20\mu m$). Specifically, in the marine ecosystem studied (Strait of Sicily), the analysis is focused on the picophytoplankton fraction, which accounts, on average, about for 80% of the total *chl a* and *Dvchl a* [4, 5, 8–10], and consists of two main domains: picoprokaryotes and picoeukaryotes. The former is composed of two genera of cyanobacteria, i.e. Synechococcus and Prochlorococcus. The latter is dominated by Prymnesiophytes, Pelagophytes and green algae. On the other hand, the nano- and micro-phytoplankton fraction accounts for about 20% of the total *chl a* and *Dvchl a* on average, and is mainly represented by the eukaryotes domain, i.e. Prymnesiophytes, Pelagophytes, Dinophytes and diatoms. This fraction is poorly present in DCM, and is almost uniformly distributed along the water column.

In this study, we analyze the behaviour of four picophytoplankton populations, i.e. Synechococcus, Prochlorococcus (HL-ecotype), Prochlorococcus (HL-ecotype) and the whole picoeukaryotes domain, which are located at different depths along the water column. Field observations indeed indicate a prevalence of Synechococcus close to the water surface, while Prochlorococcus and picoeukaryotes dominate the intermediate deeper layers [4, 5].

Synechococcus is mostly present close to the coasts, where its cell concentration reaches

usually the maximum value. Moreover, the analyses carried out along the water column showed the presence of nine different phylogenetic groups (clades) of Synechococcus in the Mediterranean Sea, most of which are observed in the Strait of Sicily [9].

The Prochlorococcus concentration is characterized by a bimodal distribution in the intermediate layers of the water column [5, 9], indicating the coexistence of two ecotypes of this genus: high light-adapted (HL-) ecotype and low light-adapted (LL-) ecotype. The former ecotype is localized in the upper part of the MAW between the surface water and 90 m of depth. The latter is mostly present at depths greater than 50 m [5, 8, 9]. Moreover, recent studies showed that the Prochlorococcus HL-ecotype prevails close to the Sicilian coast [4, 5, 9], while Prochlorococcus LL-ecotype dominates the marine ecosystem between the Sicilian - Maltese shelf and the Libyan coast [8, 9]. However, the biological features of both Prochlorococcus ecotypes can change along the Cape Passero - Misurata transect. Indeed, the phylogenetic analyses performed in the Strait of Sicily indicate the presence of two different clades of Prochlorococcus HL-ecotype in the upper layer of the water column, while three different clades of Prochlorococcus LL-ecotype were detected in deeper layers, contemporaneously. It is worth to recall that heterogenous composition is also a feature of the picoeukaryotes domain. Indeed, Brunet et al. found that Prymnesiophytes are more abundant in shallower layers of MAW, while Pelagophytes prevail in deeper layers [4, 5]. However, unlike other marine ecosystems, no previous studies confirmed a clear segregation of groups belonging to the picoeukaryotes domain in the transect investigated.

In our study, the prevalence of different clades, ecotypes and/or groups inside the four picophytoplankton populations, whose dynamics is modeled in this work, is taken into account for each hydrological station of the Cape Passero - Misurata transect. In particular, we use different settings for some biological parameters, such as the half-saturation constants for light intensity and nutrient concentration, in order to consider the phylogenetic modifications among the marine stations investigated.

The analysis of seawater samples shows that Synechococcus contributes on average to more than 20% of the total chlorophyll concentration in the Strait of Sicily [4, 5]. In particular, the average concentration of Synechococcus is 5.8×10^3 cell ml^{-1}, while its concentration peak (1.05×10^4 cell ml^{-1}) is localized at 50 m of depth. The *chl a* cellular content of Synechococcus has never been estimated in the Strait of Sicily. Therefore, assuming the oligotrophic conditions, we chose to use the content measured by Vaulet and Courties in the English Channel waters, whose value was fixed equal to 1.18 fg *chl a* cell^{-1} [11].

In the Strait of Sicily, Prochlorococcus and picoeukaryotes contribute equally to the primary

production in terms of *chl a* and *Dvchl a* concentrations in intermediate and deeper layers of the MAW. However, picophytoplankton is numerically dominated by Prochlorococcus with an average concentration of 5.2×10^4 cell ml^{-1}. Specifically, this group is mainly localized in DCM, where can reach the mean value of 12.5×10^4 cell ml^{-1}. The marker of Prochlorococcus is *divinil chlorophyll a*, whose molecular structure is very similar to that of *chlorophyll a*. The *Dvchl a* cellular content of total Prochlorococcus ranges between 0.25 and 2.20 fg *Dvchl a* cell^{-1} along the water column, with a mean value exponentially increasing with the depth [5].

The analysis performed on the seawaters shows that the average picoeukaryotes concentration in the DCM is 0.6×10^3 cell ml^{-1} [4, 5, 7], while the mean value of *chl a* cell^{-1} ranges between 10 and 660 fg *chl a* cell^{-1} along the water column, with a significant exponential increase with the depth [5]. Therefore, the concentration of *chl a* per picoeukaryotes cell changes within the MAW, assuming significantly higher values in the DCM respect to the upper layer [12, 13].

On the basis of these findings, we convert the picophytoplankton abundances into chlorophyll concentration by using the two conversion curves obtained by Brunet et al. [5] for Prochlorococcus and picoeukaryotes (see Fig. 2 in Supplementary Figures).

Setting of parameters

In this work, we reproduce the two-dimensional distribution of the total chlorophyll concentration experimentally observed in the Strait of Sicily, by setting the values of the environmental and biological parameters so that the monostability condition in the marine ecosystem is obtained. In particular, initially the environmental parameters are estimated by the experimental data collected along the Cape Passero - Misurata transect. Afterwards, on the basis of the environmental conditions observed along the water column, the biological parameters are fixed in such a way to guarantee the coexistence of all four planktonic populations [14–16] in the intermediate and deeper layers. By this way, we mimic the presence of a deep chlorophyll maximum (DCM) in all hydrological stations, although the peak of abundance for each group is localized at a different depth [14–18].

In accordance with the field observations, the hydrodynamical variables are fixed in the model at constant values during the whole sampling period investigated (15-30 July 2008), even if they can change during the year. Since the only field data available in this study

were those acquired during the MedSudMed-08 oceanographic survey (summer season 2008), we did not have any data to reproduce the effects of seasonal changes in hydrological variables during the whole period investigated by the model (approximately two years and three months). However, in previous works [16, 19] it has been shown that, in Mediterranean Sea, the seasonal changes of environmental parameters do not modify significantly the steady spatial distributions of phytoplankton abundance obtained in summer season, since the hydrological variables remain almost constant between late spring and late autumn. For these reasons, the stationarity assumption can be considered valid, even though the steady solution is reached after a very long integration time and the seasonal changes of environmental variables are not taken into account in the model (see main article).

The numerical values assigned to biological and environmental parameters are shown in Table I of Supplementary Tables.

In our model, we introduce some environmental parameters acquired directly in the Strait of Sicily during the summer season. Specifically, as a preliminary step, we assume that the horizontal velocity component, v_h, takes on the same direction of the meridional geostrophic velocity, v, measured in the sampling sites. This choice is correct since the Cape Passero - Misurata transect can be considered almost parallel to the Earth meridian at $15^o10'$ of east longitude. The spatial distribution of the horizontal velocity component, $v_h(x, z)$, is therefore reproduced by interpolating the vertical profiles of the meridional geostrophic velocity, $v(z)$, collected in each hydrological station, and is inserted in Eqs. (1), (2) and (5) of the model (see main article).

In this work, the vertical turbulent diffusivity is reproduced according to the method by Pacanowski and Philander [20, 21], by using the experimental profiles of geostrophic velocity components and density collected along the Cape Passero - Misurata transect. In particular, to obtain the vertical turbulent diffusivity as a function of the depth, $D_v(z)$, in each sampling site we use the following expression based on the empirical studies [20, 22, 23]:

$$D_v(z) = \frac{\nu_0}{(1 + \alpha \cdot Ri(z))^n} + \nu_b, \tag{1}$$

where $\nu_0 = 36m^2/h$, $\alpha = 5.0$, and $n = 1.0$ are adjustable parameters chosen for lower intensities of wind stress, $\nu_b = 0.36m^2/h$ is the background dissipation parameter, $Ri(z)$ is the gradient Richardson number, depending on the depth, given by

$$Ri(z) = \frac{N^2(z)}{shear^2(z)} \tag{2}$$

Here, the buoyancy frequency $N(z)$ is calculated directly by the vertical profile of water density as follows

$$N^2(z) = (g/\rho_w) \cdot \frac{\partial \rho(z)}{\partial z}, \tag{3}$$

where g is the gravity acceleration, ρ_w is the density of the sea water, and $\frac{\partial \rho(z)}{\partial z}$ is the vertical density gradient. On the other hand, the shear of the mean currents, $shear(z)$, depends on the vertical profiles of the horizontal velocity components according to the following expression [20, 21]

$$shear^2(z) = \left(\frac{\partial u(z)}{\partial z}\right)^2 + \left(\frac{\partial v(z)}{\partial z}\right)^2, \tag{4}$$

where $u(z)$ and $v(z)$ are the zonal and the meridional geostrophic current components measured along the water column in each hydrological station of the Cape Passero - Misurata transect. By this way, we get the two-dimensional distribution of the vertical turbulent diffusivity, $D_v(x, z)$, by interpolating the theoretical profiles obtained for the 12 hydrological stations.

Unlike the other environmental parameters, the horizontal turbulent diffusivity, $D_h(x)$, can not be calculated by using the experimental data collected in the Strait of Sicily. Therefore, the values of this parameter are set in agreement with the theoretical findings obtained in previous works [20, 24, 25]. In particular, in our model the horizontal turbulent diffusivity decreases from the maximum value, $D_h(x) = 36.0\ km^2/h$, (station $M1$, close to the Sicilian coast) to the minimum value, $D_h(x) = 7.2\ km^2/h$, (station $M4$, at the beginning of the Medina Sill). In the other hydrological stations the horizontal turbulent diffusivity is independent of the position x along the transect and is set to $7.2\ km^2/h$, according to theoretical results obtained by Katz et al. for deeper waters [20, 24].

The one-dimensional behaviour of the incident light intensity at the water surface ($I_{in}(x)$) is estimated by using the remote sensing data (see the NASA web site http://eosweb.larc.nasa.gov/sse/RETScreen/) acquired for each station of the transect, while the two-dimensional distribution of the phosphate concentration at the initial time ($t = 0$) is set on the basis of the analysis performed on the bottle samples collected at different depths in the hydrological stations. By this way, we also obtain the phosphate concentration at the boundaries of the two-dimensional domain, $R_{in}(x, z)$, necessary to solve the equations of the model.

The biological parameters are set to values typical of the four phytoplankton populations studied, according to previous theoretical and experimental results [4, 5, 11, 12, 18, 26–35]. In particular, the maximum specific growth rates are fixed in accordance with experimental results given in Refs. [28–30], while the specific loss rates are estimated on the basis of

experimental findings given in Refs. [28, 30–32]. On the other hand, the swimming velocity and nutrient recycling coefficients are chosen in agreement with the theoretical results obtained by other authors [27, 31]. Specifically, the magnitudes of swimming velocities of the four planktonic populations are set to the values obtained by Raven [27], while nutrient recycling coefficients are calculated by considering the assimilation efficiencies estimated by Thingstad [31].

In previous works [14–16], as well as in our preliminary analysis, the half-saturation constants of the picophytoplankton groups are fixed to the average values observed experimentally (see parameters of the full model in Table I). In particular, the half-saturation constants K_{I_i} are fixed at low values for those populations, such as picoeukaryotes and Prochlorococcus LL, which are better adapted to low light intensities. At the same time, the half-saturation constants K_{R_i} are set at low values for those populations, such as Synechococcus and Prochlorococcus HL, which are better adapted to low nutrient concentrations. Therefore, the abundance peaks of picoeukaryotes and Prochlorococcus LL are localized in the deeper layers of the MAW, while those of the Synechococcus and Prochlorococcus HL are placed in the intermediate layers.

Conversely, on the basis of the field observations, the core of this study exploits half-saturation constants set to different values in the twelve hydrological stations investigated (see parameters of the reduced model in Table I). Indeed we recall that in the Strait of Sicily the picoeukaryotes domain includes several groups [4, 5], while Synechococcus, Prochlorococcus HL and Prochlorococcus LL are characterized by the presence of different clades [8, 9]. For each phytoplankton population this biodiversity is a marker of the skills of adaptation at the different environmental conditions observed within the 2D domain of the marine ecosystem. As a consequence, depending on the marine site analyzed, different clades, ecotypes and/or groups prevail inside each population, and the half-saturation constants have to change accordingly [36]. Thus, the half-saturation constants, K_{R_i} and K_{I_i}, for the four populations are set so that the production layers and the peaks of phytoplankton abundance are placed at depths compatible with those observed by Brunet et al. [4, 5] in the Strait of Sicily. In particular, according to Ryabov et al., for the i-th population and for each hydrological station, we consider the following expressions

$$K_{R_i} = \frac{(r_i - m_i)}{m_i} R_i^* \tag{5}$$

$$K_{I_i} = \frac{(r_i - m_i)}{m_i} I_i^*, \tag{6}$$

where R_i^* and I_i^* are the critical values, defined as the values of the resource availability at the boundaries of the production layer, r_i is the maximum specific growth rate, and m_i is the specific loss rate [15, 37]. As a preliminary step, we calculate the values of half-saturation constants by using in Eqs. (5), (6) the critical values of nutrient concentration and light intensity obtained from the field data. The values of half-saturation constants estimated in this way are successively adjusted by using again Eqs. (5), (6), in which new values for R_i^* and I_i^*, calculated from the model, are used instead of those obtained from the field data. By applying iteratively this procedure, the values of half-saturation constants are refined in such a way to optimize the chlorophyll distributions obtained from the model compared with the experimental profiles.

Conversely, the nutrient contents of the planktonic populations, $1/Y_i$, are fixed to the same values for all hydrological stations (see Table I). Specifically, the values of these parameters are estimated for Synechococcus and picoeukaryotes according to the experimental findings obtained in previous works [34, 35], while no data are available for any Prochlorococcus ecotype (neither HL, nor LL). Therefore, in order to get phytoplankton abundances in accordance with the experimental results, we fix the nutrient content of the Prochlorococcus (both ecotypes) in such a way to respect the ratios of the average concentrations of the planktonic groups experimentally observed in the Strait of Sicily [4, 5].

Finally, the *chl a*-normalized average absorption coefficients are calculated on the basis of the light absorption spectra obtained for phytoplankton cultures by Hickman et al. [16, 18]. In general, the values estimated are in agreement with the absorption coefficients measured by Brunet et al. in the coastal zones of the Mediterranean Sea [12, 13].

Statistical analysis

Since some parameters (seven half-saturation constants) are freely estimated in the model, it is worth to investigate the real goodness of the fit obtained by performing a comparison, based on the χ^2 test, between the reduced model and the full model [39]. Specifically, in order to establish which of them reproduces better the field data, we applied for both models the Akaike Information Criterion (AIC) [38, 39] defined as follows

$$AIC(H) = \chi^2_{df} - df, \tag{7}$$

where χ^2_{df} denotes a chi-squared with a number of degrees of freedom, df, equal to the

number of independent constraints of the model, H. The minimum value of AIC indicates the model with the best fit.

In Table II, we show the AIC statistics calculated for each hydrological station and the whole transect. Here, the results indicate that the best AIC in the most sites (eleven hydrological stations over twelve) is obtained by the full model, while the χ^2 test show that the best fit is usually observed by using the reduced model. However, for the whole transect we observe that the best AIC statistics is obtained by using the reduced model, in accordance with the result of the χ^2 test.

Therefore, on this basis the reduced model seems to be the best tool to reproduce the overall two-dimensional distribution of chlorophyll concentration. On the other hand, the full model is able to well reproduce the experimental chlorophyll profiles in the most sites of the transect.

This conclusion can be further checked by using an other statistical tool, which defines a magnitude difference between the chi-square for the reduced model and the chi-square for the full model. In particular, we estimate this magnitude difference by using the Cohen's effect size measure [39]

$$w = (\triangle\chi^2_{df}/(N \cdot \triangle df))^{0.5}, \tag{8}$$

where N is the sample size, equal for both models, $\triangle\chi^2_{df}$ is the difference in chi-square and $\triangle df$ the difference in degrees of freedom between the two models.

According to the Cohen's suggested standard for a small effect ($w \leq 0.1$) [39], the value obtained for the index w indicates that using the reduced model affects weakly (see Table II of Supplementary Tables) the result of the χ^2 test in the whole transect ($w = 0.08$). Specifically, according to the values of w, the decrease of χ^2 is negligible in the sites from $M4$ to $M12$, while it is more significative, although still small, in the three hydrological stations localized close to the Sicilian coast. On the whole, the reduced model therefore allows to improve the results of the χ^2 test compared to the full model, even if this improvement is not actually very significative.

SUPPLEMENTARY REFERENCES

[1] Placenti, F. et al. Water masses and nutrient distribution in the Gulf of Syrte and between Sicily and Libya. *J. Marine Syst.* **121–122**, 36–46 (2013).

[2] Bonanno, A. et al. Variability of water mass properties in the Strait of Sicily in summer period of 1998–2013. *Ocean Sci.* **10**, 759–770 (2014).

[3] Ribera d'Alcalà, M., Civitarese, G., Conversano, F., Lavezza, R. Nutrient ratios and fluxes hint at overlooked processes in the Mediterranean Sea. *J. Geophys. Res.* **108(C9)**, 8106 (2003).

[4] Brunet, C., Casotti, R., Vantrepotte, V., Corato, F., Conversano, F. Picophytoplankton diversity and photoacclimation in the Strait of Sicily (Mediterranean Sea) in summer. I. Mesoscale variations. *Aquat. Microb. Ecol.* **44**, 127–141 (2006).

[5] Brunet, C., Casotti, R., Vantrepotte, V., Conversano, F. Vertical variability and diel dynamics of picophytoplankton in the Strait of Sicily, Mediterranean Sea, in summer. *Mar. Ecol. Prog. Ser.* **346**, 15–26 (2007).

[6] Casotti, R., Brunet, C., Aronne, B., Ribera d'Alcalà, M. Mesoscale features of phytoplankton and planktonic bacteria in a coastal area as induced by external water masses. *Mar. Ecol. Prog. Ser.* **195**, 15–27 (2000).

[7] Casotti, R. et al. Composition and dynamics of the phytoplankton of the Ionian Sea (Eastern Mediterranean). *J. Geophys. Res.* **108(C9)**, 8116 (2003).

[8] Garczarek, L. et al. High vertical and low horizontal diversity of *Prochlorococcus* ecotypes in the Mediterranean Sea in summer. *FEMS Microbiol Ecol.* **60**, 189–206 (2007).

[9] Mella-Flores, D. et al. Is the distribution of Prochlorococcus and Synechococcus ecotypes in the Mediterranean Sea affected by global warming? *Biogeosciences* **8(9)**, 2785–2804 (2011).

[10] La Ferla, R. et al. Vertical distribution of the prokaryotic cell size in the Mediterranean Sea. *Helgol. Mar. Res.* **66(4)**, 635–650 (2012).

[11] Morel, A., Ahn, Y.H., Partensky, F., Vaulot, D., Claustre, H. *Prochlorococcus* and *Synechococcus*: A comparative study of their optical properties in relation to their size and pigmentation. *J. Mar. Res.* **51**, 617–649 (1993).

[12] Brunet, C., Casotti, R., Aronne, B., Vantrepotte, V. Measured photophysiological parameters used as tools to estimate vertical water movements in the coastal Mediterranean. *J. Plankton*

Res. **25**, 1413–1425 (2003).

[13] Brunet, C., Casotti, R., Vantrepotte, V. Phytoplankton diel and vertical variability in photobiological responses at a coastal station in the Mediterranean Sea. *J. Plankton Res.* **30**, 645–654 (2008).

[14] Huisman, J., Thi, N.N.P., Karl, D.M., Sommeijer, B. Reduced mixing generates oscillations and chaos in the oceanic deep chlorophyll maximum. *Nature* **439**, 322–325 (2006).

[15] Ryabov, A.B., Rudolf, L., Blasius, B. Vertical distribution and composition of phytoplankton under the influence of an upper mixed layer. *J. Theor. Biol.* **263**, 120–133 (2010).

[16] Valenti, D., Denaro, G., Spagnolo, B., Conversano, F., Brunet, C. How diffusivity, thermocline and incident light intensity modulate the dynamics of deep chlorphyll maximum in Tyrrhenian Sea. *PLoS ONE* **10(1)**, e0115468 (2015).

[17] Klausmeier, C.A., Litchman, E. Algal games: the vertical distribution of phytoplankton in poorly mixed water columns. *Limnol. Oceanogr.* **46**, 1998–2007 (2001).

[18] Hickman, A., Dutkiewicz, S., Williams, R., Follows, M. Modelling the effects of chromatic adaptation on phytoplankton community structure in the oligotrophic ocean. *Mar. Ecol. Prog. Ser.* **406**, 1–17 (2010).

[19] Valenti, D. et al. Stochastic models for phytoplankton dynamics in Mediterranean Sea. *Ecol. Complex.* **27**, 84–103 (2016).

[20] Pacanowski, R.C., Philander, S.G.H. Parameterization of Vertical Mixing in Numerical Models of Tropical Oceans. *J. Phys. Oceanogr.* **11**, 1443–1451 (1981).

[21] Peters, H., Gregg, M.C., Toole, J.M. On the parameterization of Equatorial Turbulence. *J. Geophys. Res.* **93**, 1199–1218 (1988).

[22] Robinson, A.R. An investigation into the wind as the cause of the Equatorial Undercurrent. *J. Mar. Res.* **24**, 179–204 (1966).

[23] Jones, J.H. Vertical mixing in the Equatorial Undercurrent. *J. Phys. Oceanogr.* **3**, 286–296 (1973).

[24] Katz, E.J., Bruce, J.G., Petrie, B.D. Salt and mass flux in the Atlantic Equatorial Undercurrent. *Deep-Sea Res.* **26**, 139–160 1979.

[25] Massel, S.R. Fluid Mechanics for Marine Ecologists. (Springer-Verlag, Berlin Heidelberg, 1999).

[26] Morel, A. Consequences of a Synechococcus bloom upon the optical properties of oceanic (case 1) waters. *Limnol. Oceanogr.* **42(8)**, 1746–1754 1997.

[27] Raven, J.A., The twelfth tansley lecture. Small is beautiful: the picophytoplankton. *Funct.*

Ecol. **12**, 503–513 (1998).

[28] Raven, J.A., Finkel, Z.V., Irwin, A.J. Picophytoplankton: bottom-up an top-down controls on ecology and evolution. *J. Geophys. Res.* **55**, 209–215 (2005).

[29] Dimier, C., Brunet, C., Geider, R., Raven, J. Growth and photoregulation dynamics of the picoeukaryote *Pelagomonas calceolata* in fluctuating light. *Limnol. Oceanogr.* **54**, 823–836 (2009).

[30] Veldhuis, M.J.W., Timmermans, K.R., Croot, P., Van Der Wagt, B. Picophytoplankton; a comparative study of their biochemical composition and photosynthetic properties. *J. Sea Res.* **53**, 7–24 (2005).

[31] Thingstad, T.F., Sakshaugh, E. Control of phytoplankton growth in nutrient recycling ecosystems. Theory and terminology. *Mar. Ecol. Prog. Ser.* **63**, 261–272 (1990).

[32] Quevedo, M., Anadón, R. Protist control of phytoplankton growth in the subtropical northeast Atlantic. *Mar. Ecol. Prog. Ser.* **221**, 20–38 (2001).

[33] Moore, L.R., Goericke, R., Chisholm, S.W. Comparative physiology of synechococcus and prochlorococcus: influence of light and temperature on growth, pigments, fluorescence and absorptive properties. *Mar. Ecol. Prog. Ser.* **116**, 259–275 (1995).

[34] Bertilsson, S., Berglund, O., Karl, D.M., Chisholm, S.W. Elemental composition of marine *Prochlorococcus* and *Synechococcus*: implications for the ecological stoichiometry of the sea. *Limnol. Oceanogr.* **48**, 1721–1731 (2003).

[35] Timmermans, K.R., van der Wagt, B., Veldhuis, M.J.W., Maatman, A., de Baar, H.J.W. Physiological responses of three species of marine pico-phytoplankton to ammonium, phospahte, iron and light limitation. *J. Sea Res.* **53**, 109–120 (2005).

[36] Moon-Van Der Staay, S.Y., De Wachter, R., Vaulot, D. Oceanic 18S rDNA sequences from picoplankton reveal unsuspected eukaryotic diversity. *Nature* **409**, 607–610 (2001).

[37] Ryabov, A. Phytoplankton competition in deep biomass maximum. *Theor. Ecol.* **5**, 373–385 (2012).

[38] Akaike, H. Factor analysis and AIC. *Psychometrika* **52**, 317–332 (1987).

[39] Newsom, J.T. *Longitudinal Structural Equation Modeling: A Comprehensive Introduction* (Routledge, New York, NY, 2015).

SUPPLEMENTARY TABLES

Symbol	Interpretation	Units	Reduced Model	Full Model
a_{bg}	Background turbidity	m^{-1}	0.060	0.060
a_1	Average absorption coefficient of Synechococcus	m^2 mg chl-a $^{-1}$	0.025	0.025
a_2	Average absorption coefficient of Prochlorococcus HL	m^2 mg chl-a $^{-1}$	0.016	0.016
a_3	Average absorption coefficient of picoeukaryotes	m^2 mg chl-a $^{-1}$	0.012	0.012
a_4	Average absorption coefficient of Prochlorococcus LL	m^2 mg chl-a $^{-1}$	0.027	0.027
a_6	Average absorption coefficient of phytoplankton $> 3\mu m$	m^2 mg chl-a $^{-1}$	0.020	0.020
r_1	Maximum specific growth rate of Synechococcus	h^{-1}	0.058	0.058
r_2	Maximum specific growth rate of Prochlorococcus HL	h^{-1}	0.088	0.088
r_3	Maximum specific growth rate of picoeukaryotes	h^{-1}	0.096	0.096
r_4	Maximum specific growth rate of Prochlorococcus LL	h^{-1}	0.031	0.031
K_{I_1}	Half-saturation constant of light-limited growth of Synechococcus (as a function of distance)	μmol photons m^{-2} s^{-1}	12.50 – 130.00	130.00
K_{I_2}	Half-saturation constant of light-limited growth of Prochlorococcus HL (as a function of distance)	μmol photons m^{-2} s^{-1}	24.50 – 80.00	80.00
K_{I_3}	Half-saturation constant of light-limited growth of picoeukaryotes (as a function of distance)	μmol photons m^{-2} s^{-1}	16.50 – 67.50	67.50
K_{I_4}	Half-saturation constant of light-limited growth of Prochlorococcus LL (as a function of distance)	μmol photons m^{-2} s^{-1}	0.01 – 24.50	1.00
K_{R_1}	Half-saturation constant of nutrient-limited growth of Synechococcus	mmol phosphorus m^{-3}	0.000	0.000
K_{R_2}	Half-saturation constant of nutrient-limited growth of Prochlorococcus HL (as a function of distance)	mmol phosphorus m^{-3}	0.000 – 0.365	0.060
K_{R_3}	Half-saturation constant of nutrient-limited growth of picoeukaryotes (as a function of distance)	mmol phosphorus m^{-3}	0.000 – 1.000	0.098
K_{R_4}	Half-saturation constant of nutrient-limited growth of Prochlorococcus LL (as a function of distance)	mmol phosphorus m^{-3}	0.000 – 0.095	0.040
m_1	Specific loss rate of Synechococcus	h^{-1}	0.014	0.014
$m_2 = m_4$	Specific loss rate of Prochlorococcus	h^{-1}	0.011	0.011
m_3	Specific loss rate of picoeukaryotes	h^{-1}	0.010	0.010
$1/Y_1$	Nutrient content of Synechococcus	mmol phosphorus $cell^{-1}$	2.0×10^{-12}	2.0×10^{-12}
$1/Y_2 = 1/Y_4$	Nutrient content of Prochlorococcus	mmol phosphorus $cell^{-1}$	4.0×10^{-13}	4.0×10^{-13}
$1/Y_3$	Nutrient content of picoeukaryotes	mmol phosphorus $cell^{-1}$	2.00×10^{-12}	2.00×10^{-12}
c_1	Chl-a cellular content of Synechococcus	fg chl-a $cell^{-1}$	1.18	1.18
c_3	Chl-a cellular content of picoeukaryotes (as a function of depth)	fg chl-a $cell^{-1}$	10.00 – 660.00	10.00 – 660.00
$c_2 = c_4$	Dvchl-a cellular content of Prochlorococcus (as a function of depth)	fg Dvchl-a $cell^{-1}$	0.25 – 2.20	0.25 – 2.20
ε_1	Nutrient recycling coefficient of Synechococcus	dimensionless	0.51	0.51
$\varepsilon_2 = \varepsilon_4$	Nutrient recycling coefficient of Prochlorococcus	dimensionless	0.52	0.52
ε_3	Nutrient recycling coefficient of picoeukaryotes	dimensionless	0.52	0.52
v_1^s	Magnitude of swimming velocity of Synechococcus	m h^{-1}	0.000088	0.000088
$v_2^s = v_4^s$	Magnitude of swimming velocity of Prochlorococcus	m h^{-1}	0.000039	0.000039
v_3^s	Magnitude of swimming velocity of picoeukaryotes	m h^{-1}	0.000098	0.000098
D_V	Vertical turbulent diffusivity (as a function of depth and distance)	m^2 h^{-1}	0.360 – 22.08	0.360 – 22.08
D_H	Horizontal turbulent diffusivity (as a function of distance)	km^2 h^{-1}	7.2 – 36.0	7.2 – 36.0
z_b	Depth of the water column (as a function of distance)	m	50 – 200	50 – 200
R_{in}	Nutrient concentration at the domain boundaries	mmol phosphorus m^{-3}	0.010 – 0.110	0.010 – 0.110

TABLE I: Parameters used for reduced and full model. The values of the biological and environmental parameters are those typical of four picophytoplankton populations that coexist in the Strait of Sicily.

Station	χ^2_{red}	$\tilde{\chi}^2_{red}$	χ^2_{ful}	$\tilde{\chi}^2_{ful}$	AIC_{red}	AIC_{ful}	w
$M1$	1.27	0.0508	6.55	0.2620	-68.73	-77.45	0.17
$M2$	1.63	0.0271	23.44	0.3904	-68.37	-60.58	0.23
$M3$	0.64	0.0112	11.57	0.2029	-69.36	-72.43	0.17
$M4$	1.19	0.0145	1.96	0.0239	-68.81	-82.04	0.04
$M5$	1.19	0.0120	2.71	0.0274	-68.81	-81.29	0.05
$M6$	0.43	0.0059	1.06	0.0145	-69.57	-82.94	0.04
$M7$	1.00	0.0100	0.84	0.0084	-69.00	-83.16	0.02
$M8$	0.72	0.0072	0.83	0.0083	-69.28	-83.17	0.01
$M9$	1.12	0.0113	5.07	0.0512	-68.88	-78.93	0.08
$M10$	1.52	0.0152	0.47	0.0047	-68.48	-83.53	0.04
$M11$	1.99	0.0199	1.84	0.0184	-68.01	-82.16	0.01
$M12$	0.11	0.0021	0.39	0.0079	-69.89	-83.61	0.03
$Transect$	12.80	0.0136	56.70	0.0600	-57.20	-27.30	0.08

TABLE II: Results of χ^2 test, reduced chi-square ($\tilde{\chi}^2$) test, Akaike Information Criterion (AIC), and Cohen's effect size measure (w) for the twelve hydrological stations and the whole transect investigated. All statistical tests are carried out for the reduced model (χ^2_{red}, $\tilde{\chi}^2_{red}$ and AIC_{red}) and the full model (χ^2_{ful}, $\tilde{\chi}^2_{ful}$ and AIC_{ful}). The Cohen's effect size measure (w) is calculated on the basis of χ^2 tests, according to Eq.(8). The number of samples, used for the test and distanced of 2 m, depends on the depth of the MAW in each station.

SUPPLEMENTARY FIGURES

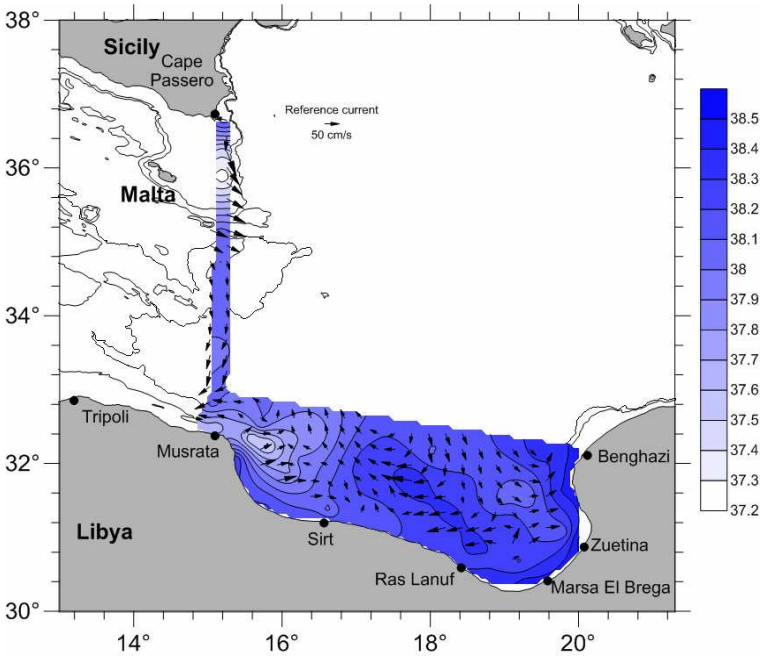

FIG. 1: Horizontal distribution of interpolated LADCP current velocities and minimum of salinity in the upper layer (10 - 80 m). Map was obtained by Surfer [12] from Golden Software, LLC (www.goldensoftware.com).

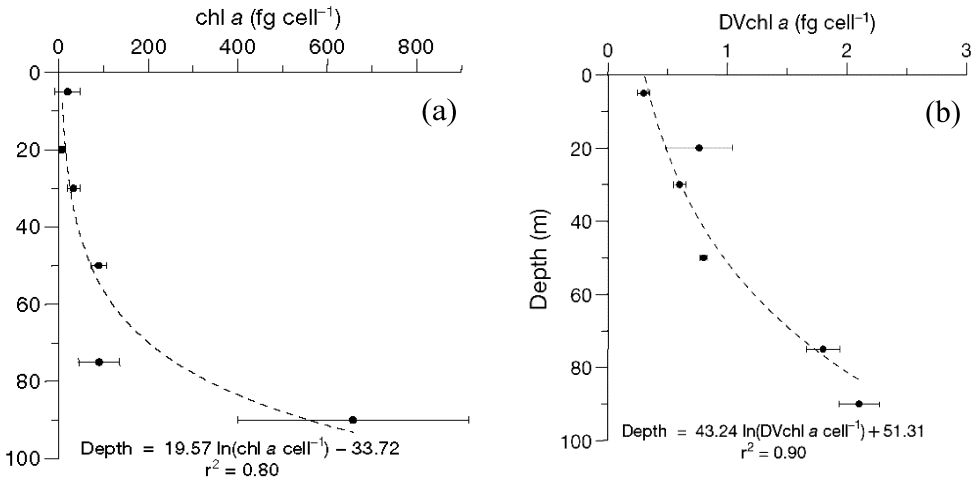

FIG. 2: Mean vertical profile of *chl a* per picoeukaryote cell (panel a) and *Dvchl a* per Prochlorococcus cell (panel b). Error bars are Standard Deviation. Equation and r^2 for the fit are reported on the plots. (Courtesy of Brunet et al., 2007 (Ref. [5])).